WIND TUNNEL TESTS ON A SECTIONAL MODEL OF THE AUCKLAND HARBOUR BRIDGE CYCLEWAY, AUCKLAND

By

s 9(2)(a)

and

s 9(2)(a)

SUMMARY

Wind tunnel tests have been carried out on a sectional model of the proposed Auckland Harbour Bridge Cycleway in turbulent flow to determine the sectional mean force and moment characteristics and aerodynamic damping properties over a range of angles of attack between -10 degrees and +15 degrees. Due to the interaction with the existing Auckland Harbour Bridge (AHB), the rigid sectional model was tested in six Section Studies, outlined as follows:

- Section Study 1 – Span 2 located upstream of the existing AHB
- Section Study 2 – Span 2 located downstream of the existing AHB
- Section Study 3 – Span 4 located upstream of the existing AHB
- Section Study 4 – Span 4 located downstream of the existing AHB
- Section Study 5 – Viewing Platform located upstream of the existing AHB
- Section Study 6 – Viewing Platform located downstream of the existing AHB

The proposed design was found to suffer from aerodynamic instability, so further investigations were commissioned and performed to investigate aerodynamic strategies to achieve stability. In addition, modifications were made to the structural design of the Cycleway to increase the modal frequencies. BECA have opted for strategies that include aerodynamic modifications and damping to achieve stability for wind speeds up to and just above ULS. BECA have indicated they will ensure a minimum damping of 5% of critical (structural + damper). The mean force and moment coefficients for all Cycleway Section Studies have been determined and presented for this modified design. The aerodynamic damping for Section Studies 1 to 4 have been determined and presented for the modified design.

For mean force and moment characteristics, Section Studies with the Cycleway upstream of the existing AHB structure were found to be most critical. The data show that there is little significant difference in the mean force and moment coefficients, between Section Studies 1 and 3. The trend of the Lift Coefficients, C_L, in these Section Studies show a generally positive lift slope across the range of angles of attack tested. Variation in Drag Coefficients, C_D, with changing angle of attack is shown to fall between 1.6 and 0.8 for both Section Studies 1 and 3. Similarly, the Moment Coefficients, C_M, in these two Section Studies have been shown to be positive for all angles of attack, ranging from 0.75 to 0.35.

The data show that the mean force and moment coefficients for the Viewing Platform are more critical for Section Study 5. The Lift Coefficients, C_L, are shown to exhibit a positive lift slope across the range of angles tested. The mean Drag Coefficients, C_D, are shown to range from 2.6 to 1.8. The mean Moment Coefficients, C_M, show a decreasing trend as the angle of attack moves away from 0 degrees, ranging between 1 to 1.55.

The lift aerodynamic damping of the proposed AHB Cycleway has been determined and presented for all angles of attack and range of Reduced Velocities including Serviceability Limit State (SLS) and Ultimate Limit State (ULS). This has been shown to be negative for all angles of attack for both Section Studies, to reach a highest negative aerodynamic damping of -4.5%.

The Gust Factors and C_{dyn} Factors have been provided to account for the correlation of the drag loads for each pier.

It is recommended that the full aeroelastic bridge wind tunnel model study be undertaken to assess the aerodynamic performance of the Cycleway.

Report 92-19-WT-SEC-01
June 2020

AUCKLAND HARBOUR BRIDGE CYCLEWAY – AUCKLAND, NZ
WIND TUNNEL SECTIONAL STUDY

MEL CONSULTANTS REPORT NO: **92-19-WT-SEC-01**

PREPARED FOR:
BECA
21 Pitt Street
Auckland 1010
New Zealand

Contact:
s 9(2)(a)

PREPARED BY:
MEL Consultants Pty Ltd
22 Cleeland Road
Oakleigh South VIC 3167

Contact:
s 9(2)(a)

PREPARED BY:
s 9(2)(a)
Date: 17 June 2020

REVIEWED BY:
s 9(2)(a)
Date: 17 June 2020

RELEASED BY:
s 9(2)(a)
Date: 18 June 2020

REVISION HISTORY

Revision No:	Date Issued	Reason/Comment
0	5 March 2020	Initial Issue
1	18 June 2020	Review Update

DISTRIBUTION

Copy No:
1

Copy	Location	Type
1	BECA	Electronic PDF
2	MEL Consultants – Report Library	Hardcopy
3	MEL Consultants – Report Library	Hardcopy
4	MEL Consultants – Project File	Hardcopy

NOTE: This is a controlled document within the document control system. If revised, it must be marked SUPERSEDED and returned to the MEL Consultants Pty Ltd contact.

CONTENTS

1 INTRODUCTION

The Auckland Harbour Bridge Cycleway will be a bicycle and pedestrian bridge located on the outboard side of the southbound extension of the Auckland Harbour Bridge (AHB). The AHB spans approximately one kilometre between Northcote Point and Westhaven across the Waitemata Harbour. The proposed design is to have a main span (Span 2) of approximately 244m between Piers 1 and 2 with a nominal deck width of 5.5m and is 40m above the water. To understand the wind loads on the proposed Cycleway in the windward and leeward positions, sectional wind tunnel measurements were commissioned by BECA.

The scope of the study was to measure the mean drag (C_D), mean lift (C_L), and mean moment (C_M) and the aerodynamic damping of the proposed Cycleway in the presence of the existing truss and box girder bridges in the upstream and downstream positions. Outside the scope of this study is the study of the aerodynamic effects of the proposed Cycleway on the existing bridges.

The proposed Cycleway deck cross section was found to suffer from aerodynamic instability within the design wind speed range. Further testing to find a stable solution was therefore commissioned and will be included in this report.

This report describes the wind tunnel tests of a rigid sectional model of the modified bridge spans in four Section Studies which are as follows:

- Section Study 1 – Span 2 located upstream of the existing AHB
- Section Study 2 – Span 2 located downstream of the existing AHB
- Section Study 3 – Span 4 located upstream of the existing AHB
- Section Study 4 – Span 4 located downstream of the existing AHB
- Section Study 5 – Viewing Platform located upstream of the existing AHB
- Section Study 6 – Viewing Platform located downstream of the existing AHB

These tests were carried out in the Sectional Testing area in the MEL Consultants 400kW Boundary Layer Wind Tunnel during late February, 2020.

2 MODEL AND EXPERIMENTAL TECHNIQUES

2.1 Sectional Test Rig

A test apparatus for sectional model studies has been designed and built by MEL Consultants Pty Ltd. Independent systems for drag and lift forces and pitching moments have been incorporated into the system. The deck section to be tested was connected to a support on each side of the tunnel that allowed the angle of attack to be adjusted by a rotating disk and clamping arrangement. Therefore, the experimental rig maintained the principle measurement axes of the bridge motion aligned with the bridge for all angles of attack.

The deflections in the lift, drag and torsional directions were measured using laser displacement sensors that were calibrated to give forces and moments. The lasers were installed on both sides of the sectional model (six lasers) and this allowed quality checking of the movement of the section model in each direction. The displacements at each end of the bridge were cross checked for instrumentation consistency. The use of non-contact laser displacement sensors means the stiffness and damping of the bridge were not affected by the instrument system. The support and instrumentation systems allow the measurement of the dynamic forces in the drag, lift, and rotational directions.

The structural damping (% of critical) of the sectional model was changed by oil dashpots at both ends of the model. The configuration of the dampers was the same at both ends of the model. Damping (% of critical) has a 1 to 1 scaling with full scale.

2.2 Sectional Model

A model of a typical span of the proposed Cycleway was constructed at a length scale (L_r) of 1/40. The span of the sectional model was 1.95m between end plates and represented approximately 80m in full scale. The selection of the scale of the sectional model is a compromise between Reynolds number and aspect ratio (length to nominal deck width) and MEL Consultants have considered these in the selection of the length scale. Research studies have shown that it is necessary to have an aspect ratio of at least 8 to for two dimensional sectional models to ensure walls effects are negligible. As the aspect ratio decreases below 8 research has shown that the wall effects on the sectional model data becomes increasingly affected by the presence of the wind tunnel walls. Therefore, this was used to define the length scale of the model.

The wind tunnel model for Spans 2 and 4 were constructed to the drawings provided by BECA dated up to February, 2020. A sectional model is rigid, i.e. the model frequencies are well above the scaled structural frequencies of interest, so the models of Spans 2 and 4 were constructed from carbon fibre rectangular hollow section with foam attachments to create the aerodynamic shape of the bridges. These foam attachments were constructed from CNC routed foam sections, and the edge barriers/safety screens were modelled using laser cut acrylic and cardboard. The rigid sectional model of the Viewing Platform was modelled using the carbon fibre rectangular hollow section, with CNC routed foam attachments for the aerodynamic shape of the platform at the pier connection, and a 3D printed sunshade and safety screen. The experimental models and Wind Tunnel setups are shown in Figures 1 to 4.

The existing bridges were constructed based on information received for the previous sectional wind tunnel model studies of the traffic box girder bridge. This included scanned versions of the original drawings of the existing truss bridge. Since the assessment of the aerodynamic effects on the existing bridges was outside the scope of the present work these bridges were rigidly mounted in position (no dynamics), which is the same methodology used in the previous sectional model wind tunnel studies of the traffic box girder bridge. The existing bridges were rotated to be at the same angle of attack as the Cycleway sectional model during the studies.

The initial wind tunnel studies of the proposed Cycleway design identified that the bridge would suffer from aerodynamic instability, i.e. negative aerodynamic damping, and modifications were investigated to determine strategies to improve the stability of the design. These strategies were provided to the design team to assist with decisions for the bridge revised design. A brief list of designs tested (excluding combinations) to determine a stable aerodynamic design are outlined below:

1. Altered porosity of safety barriers/balustrades
2. Modifications made to the shape of underside/leading edge (e.g.: rounding of the underside, adding a ‘bullnose’ to the leading face)
3. Modification of the shape of the leading safety barrier/balustrade
4. Adding vorticity generators (e.g.: fins, lips, alternate meshing), in different orientations to the leading and trailing edges of the sectional model

The final direction provided by BECA for the section deck studies included aerodynamic modifications and the use of critical damping of 5% or greater (structural + damper). It included the original fairing design with an increased frequency in the critical direction and a curved leading safety barrier with a porosity of 60%. The final design has been detailed in Figure 5 which includes the axis notation.

2.3 Parameter Definitions and Test Procedures

Two types of measurements to obtain coefficient data were carried out with the sectional models:

1. Mean force and moment coefficients
2. Aerodynamic damping coefficients

The Drag, Lift and Moment Coefficients are defined as follows:

$$C_D = \frac{D}{\frac{1}{2}\rho \bar{V}^2 b \ell}$$

$$C_L = \frac{L}{\frac{1}{2}\rho \bar{V}^2 b \ell}$$

$$C_M = \frac{M}{\frac{1}{2}\rho \bar{V}^2 b^2 \ell}$$

where

D	is drag force along the wind direction
L	is lift force normal to the wind direction
M	is the pitching moment defined in Figure 5
ρ	density of air (1.2 kg/m^3)
$\bar{V}$	mean wind velocity at deck height (ms^{-1})
b	deck width defined in Figure 5 (Note: all coefficients normalised by deck width)
ℓ	sectional model deck length (ℓ = 1.95m)

The force and moment coefficient data are presented as a function of angles of attack between -10 to +15 degrees. The angle of attack was changed by unclamping the disk apparatus and rotating the bridge section to the desired angle measured with an inclinometer after each setting.

A static calibration was conducted by applying known weights to the deck sections. Loads for lift were applied directly and moments and the horizontal loads (drag) were applied with a string and pulley arrangement. A zero reading for the lasers and strain gauge balances were taken at the start and end of each measurement run.

The mean force and moment measurements were conducted in turbulent flow with a turbulence intensity of 3.4%. The spectral energy of the model turbulence is equivalent to the full-scale spectral energy at scales below 5m, implying an effective full-scale turbulence intensity for this bridge deck of approximately 20%. Measurements of the mean flow wind speeds and turbulence intensity were measured during each data collection run using a Cobra probe mounted upstream and slightly below the models. Most data runs were taken at wind speeds from 6 to 30 ms^{-1} covering a range of Reduced Velocities from below serviceability to above ultimate limit state velocities.

Aerodynamic damping was obtained from the difference between damping measured with the wind on minus the damping with the wind off, i.e. for a given mode the aerodynamic damping is the total damping under wind action for a given Reduced Velocity minus the structural damping for that mode with no wind.

Total damping measurements were made in turbulent flow conditions with a turbulence intensity of 3.4%. The model was excited in a single degree of freedom, i.e. one mode. The rig allowed the vertical and rotational motions to be unrestrained, but the horizontal (drag) motion was restrained. Damping values were obtained from the time histories of the damped excitation, and are given as a percentage of critical damping, ζ, defined by;

$$\zeta = \frac{1}{2\pi} ln\left(\frac{x_n}{x_{n+m}}\right)$$

where

x is the displacement

An example of a damping curve obtained from the sectional model is shown in Figure 6. The damping was determined for each mode by bandpassing the timeseries data. Figure 6 illustrates the accuracy that the damping determined, ± 0.05%.

The aerodynamic damping coefficients are presented as a function of Reduced Velocity for a range of angles of attack. The Reduced Velocity is defined as follows;

$$V_R = \frac{\bar{V}}{fb}$$

where

f is the modal frequency

The natural frequencies and mode shapes from the finite element modelling of the AHB Cycleway, as provided by BECA are as follows;

	Full Scale	
Mode	**Span 2 - Frequency (Hz)**	**Span 4 - Frequency (Hz)**
First Vertical	0.34	0.88
First Lateral	0.29	0.97
First Torsional	6.20	17.20

To scale these frequencies to model scale, a Reduced Velocity is used and defined by;

$$V_R = \frac{V_m}{f_m b_m} = \frac{V_{fs}}{f_{fs} b_{fs}}$$

Where V_m and V_{fs} are the model and full-scale velocities, f_m and f_{fs} are the model and full-scale natural frequencies in a particular mode, and b_m and b_{fs} are the model and full-scale width of the bridge deck. The model frequencies are as follows;

	Model Scale	
Mode	**Span 2 - Frequency (Hz)**	**Span 4 - Frequency (Hz)**
First Vertical	6.1	6.1
First Lateral	8.1	8.1
First Torsional	14.5	14.5

The sectional model is supported by springs that are tuned to the scaled frequencies and Figures 7 and 8 present spectra of the sectional model frequencies. Due to the support system the model frequencies are easily identified. It is noted that the same model frequencies were used for both spans and this was done for the efficient testing and the Reduced Velocity was matched by changing the wind speed range of the testing.

For this study the width was taken as follows (full-scale dimensions):

Deck Width	5.5m
Bridge Height (water height to deck, for span 2)	46.0m

Based on the modal frequencies for the proposed Cycleway and AS1170.2 design wind speeds for the bridge deck height in Terrain Category 1.5 and Terrain Category 3 wind flow. The Reduced Velocities for ULS (1000 year return period) and SLS (25 year return period) are:

SPAN 2	$\bar{V}_{1000year\ 46m\ TC1.5}$	$\bar{V}_{1000year\ 46m\ TC3}$	$\bar{V}_{25year\ 46m\ TC1.5}$	$\bar{V}_{25year\ 46m\ TC3}$
Deck Wind Speed (ms^{-1})	36.5	21.5	29.4	17.3
Reduced Velocities				
First Vertical	19.5	11.5	15.7	9.2
First Lateral	22.9	13.5	18.4	10.8
First Torsional	1.1	0.6	0.9	0.5

SPAN 4	$\bar{V}_{1000year\ 40m\ TC1.5}$	$\bar{V}_{1000year\ 40m\ TC3}$	$\bar{V}_{25year\ 40m\ TC1.5}$	$\bar{V}_{25year\ 40m\ TC3}$
Deck Wind Speed (ms^{-1})	36.5	21.5	29.4	17.3
Reduced Velocities				
First Vertical	7.5	4.4	6.1	3.6
First Lateral	6.8	4.0	5.5	3.2
First Torsional	0.4	0.2	0.3	0.2

3 DISCUSSION OF RESULTS

A displacement response time series of the proposed Cycleway design has been included to aid in the understanding of the aerodynamic instability experienced by the rigid sectional model. This is illustrated in Figure 9, showing the free vibration oscillation of the deck section to the unstable response.

3.1 Mean force and moment coefficients

The measurements of the basic mean force and moment coefficients C_L, C_D, and C_M for all testing Section Studies are shown in Figures 10 to 27 as a function of actual angles of attack, from -10 degrees to +15 degrees at 5-degree increments. Mean force and moment coefficients are presented as a function of actual angle of attack due to the induced rotation of the span subject to wind.

3.1.1 Section Study 1: Span 2 – Cycleway upstream of existing AHB

The mean Lift Coefficients, C_L, for Section Study 1 are shown in Figure 10. The data show a generally increasing C_L from -10 degrees through to +15 degrees angle of attack, from -0.8 to 0.8.

The mean Drag Coefficients, C_D, for Section Study 1 are shown in Figure 11. The data show that the C_D is decreasing as the angle of attack tends away from 0 degrees, varying from 1.5 at 0 degrees to 0.8 at -10 degrees.

The mean Moment Coefficients, C_M, for Section Study 1 are shown in Figure 12. The data show a positive C_M for all angles of attack, varying from 0.35 at 15 degrees to 0.75 at an angle of 0 degrees. The Moment Coefficients have been shown to exhibit a decreasing trend as the angle of attack tends away from 0 degrees.

3.1.2 Section Study 2: Span 2 – Cycleway downstream of existing AHB

The mean Lift Coefficients, C_L, for Section Study 2 are shown in Figure 13. The data show a generally increasing C_L from -10 degrees through to +15 degrees angle of attack, from -0.1 to 0.3.

The mean Drag Coefficients, C_D, for Section Study 2 are shown in Figure 14. The data show that the C_D is increasing as the angle of attack tends away from 0 degrees, varying from 0.1 at 0 degrees to 0.25 at -10 degrees.

The mean Moment Coefficients, C_M, for Section Study 2 are shown in Figure 15. The data show a negative C_M for all angles of attack, varying from -0.25 at -10 degrees to 0.025 at 15 degrees. The Moment Coefficients have been shown to exhibit an increasing trend as the angle of attack moves from -10 degrees to 15 degrees.

3.1.3 Section Study 3: Span 4 – Cycleway upstream of existing AHB

The mean Lift Coefficients, C_L, for Section Study 3 are shown in Figure 16. The data show a generally increasing C_L from -10 degrees through to +15 degrees angle of attack, from -0.7 to 0.8.

The mean Drag Coefficients, C_D, for Section Study 3 are shown in Figure 17. The data show that the C_D is decreasing as the angle of attack tends away from 0 degrees, varying from 1.6 at 0 degrees to 0.9 at -10 degrees.

The mean Moment Coefficients, C_M, for Section Study 3 are shown in Figure 18. The data show a positive C_M for all angles of attack, varying from approximately 0.35 at 15 degrees to 0.7 at an angle of 0 degrees. The Moment Coefficients have been shown to exhibit a decreasing trend as the angle of attack tends away from 0 degrees.

3.1.4 Section Study 4: Span 4 – Cycleway downstream of existing AHB

The mean Lift Coefficients, C_L, for Section Study 4 are shown in Figure 19. The data show a generally increasing C_L from -10 degrees through to +15 degrees angle of attack, from -0.08 to 0.13.

The mean Drag Coefficients, C_D, for Section Study 4 are shown in Figure 20. The data show that the C_D is increasing as the angle of attack tends away from 0 degrees, varying from 0.05 at 0 degrees to 0.35 at 15 degrees.

The mean Moment Coefficients, C_M, for Section Study 4 are shown in Figure 21. The data show that the C_M varies from -0.3 at -10 degrees to 0.075 at 15 degrees. The Moment Coefficients have been shown to exhibit an increasing trend as the angle of attack moves from -10 degrees to 15 degrees.

3.1.5 Section Study 5: Viewing Platform upstream of existing AHB

The mean Lift Coefficients, C_L, for Section Study 5 are shown in Figure 22. The data show a generally increasing C_L from -10 degrees through to +15 degrees angle of attack, from 0.35 to 1.4.

The mean Drag Coefficients, C_D, for Section Study 5 are shown in Figure 23. The data show that the C_D is decreasing as the angle of attack tends away from 0 degrees, varying from 2.6 at 0 degrees to 1.8 at -10 degrees.

The mean Moment Coefficients, C_M, for Section Study 5 are shown in Figure 24. The data show a positive C_M for all angles of attack, varying from 1.0 at -10 degrees to 1.55 at an angle of 0 degrees. The Moment Coefficients have been shown to exhibit a decreasing trend as the angle of attack tends away from 0 degrees.

3.1.6 Section Study 6: Viewing Platform downstream of existing AHB

The mean Lift Coefficients, C_L, for Section Study 6 are shown in Figure 25. The data show a generally increasing C_L from -10 degrees through to +15 degrees angle of attack, from -0.6 to 0.4.

The mean Drag Coefficients, C_D, for Section Study 6 are shown in Figure 26. The data show that the C_D is increasing as the angle of attack tends away from -5 degrees, varying from 0.2 at -5 degrees to 1.4 at 15 degrees.

The mean Moment Coefficients, C_M, for Section Study 6 are shown in Figure 27. The data show that the C_M varies from -0.3 at -10 degrees to 0.5 at 15 degrees. The Moment Coefficients have been shown to exhibit an increasing trend as the angle of attack moves from -10 degrees to 15 degrees.

3.2 Aerodynamic Damping

The aerodynamic damping for the first vertical modes was measured for Section Studies 1 to 4 of the modified Cycleway. Figures 28 to 31 present the aerodynamic damping for the range of angles of attack covered in these sectional studies as a function of Reduced Velocity. Testing was conducted at a range of Reduced Velocities extending beyond the SLS and ULS envelope. The figures indicate the ULS and SLS Reduced Velocity for both of the tested Section Studies of the Cycleway

The aerodynamic damping and stability were investigated for the first rotation mode. However, the box girder design of the Cycleway has resulted in a high design frequency for the first rotation mode of the deck, i.e. more than 10 times the first vertical mode. The high modal frequency resulted in very small displacements of the sectional model under wind action, which were difficult to measure. Additionally, the excitation of the deck from an initial displacement was found to transfer the energy quickly to the much lower first vertical mode frequency resulting in few rotational oscillations. Measured rotations were effectively un-measurable being down in the instrumentation noise level. However, visual observations of the deck for the first rotational mode did not detect any stability issues over the Reduced Velocity range and angles of attacked up to and just above ULS.

3.2.1 Section Study 1: Span 2 – Cycleway upstream of existing AHB

The aerodynamic damping of Section Study 1 in the vertical direction for the range of angles of attack is presented in Figure 28, as a percentage of critical damping. These data show the aerodynamic damping in this direction to be negative for all angles of attack within the envelope of the ULS and SLS Reduced Velocities, ranging from -1% to below -4.5%.

3.2.2 Section Study 2: Span 2 – Cycleway downstream of existing AHB

The aerodynamic damping of Section Study 2 in the vertical direction for the range of angles of attack is presented in Figure 29, as a percentage of critical damping. These data show the aerodynamic damping in this direction to be negative for all angles of attack within the envelope of the ULS and SLS Reduced Velocities, ranging from -0.5% to below -1.5%.

3.2.3 Section Study 3: Span 4 – Cycleway upstream of existing AHB

The aerodynamic damping of Section Study 3 in the vertical direction for the range of angles of attack is presented in Figure 30, as a percentage of critical damping. These data show the aerodynamic damping in this direction to be negative for all angles of attack within the envelope of the ULS and SLS Reduced Velocities, ranging from -1.5% to below -2.5%.

3.2.4 Section Study 4: Span 4 – Cycleway downstream of existing AHB

The aerodynamic damping of Section Study 4 in the vertical direction for the range of angles of attack is presented in Figure 31, as a percentage of critical damping. These data show the aerodynamic damping in this direction to be negative for all angles of attack within the envelope of the ULS and SLS Reduced Velocities, ranging from -1.0% to below -2.0%.

3.3 Correlation and Dynamic Factors

The Gust Factors (G) should be applied to the mean drag load that would be determined from the wind tunnel sectional model measurements and the C_{dyn} Factor should be applied to peak (gust) drag values that would be obtained from AS/NZS1170.2:2011.

The parameters used for this analysis are as follows:

- Height above water 46m
- Terrain Category 1.5
- Frequency 0.29 Hz
- Damping 5% (includes some added damping)
- Design Wind Speeds
- ULS peak gust 55.6 ms^{-1} , mean 36.4 ms^{-1}
- SLS peak gust 44.6 ms^{-1} , mean 29.3 ms^{-1}

The Gust Factors and C_{dyn} Factors have been determined for ULS and SLS wind speeds for a deck length of 420m in full (244m + 2 * (177m/2)) to determine if there is a significant difference between the ULS and SLS factors as follows:

	Gust Factors (wind tunnel data)	C_{dyn} Factors (AS/NZS1170.2:2011 data)
ULS	1.75	0.75
SLS	1.72	0.74

The Gust Factors given here are to be applied to the mean drag as determined from the wind tunnel model measurements for the ULS wind speed of 36.4ms^{-1} to give the ULS design drag loads. They are not for application to drag loads determined from AS/NZS1170.2:2011 (which are already ULS design loads based on quasi steady assumptions). No additional calculations have been done for SLS assumptions as it was shown previously that the SLS factors were similar to the ULS factors.

When considering the drag loading applied to the individual piers it would be better to be a little conservative and use a correlation length of the sum of the half spans on each side

of the pier. The correlation and dynamic effects to adjust for the section drag per unit span value to apply to the drag load at the supporting piers for ULS (1000 year return period) and SLS (25 year return period) loadings. The following table presents the ULS Gust Factors and C_{dyn} Factors for the piers.

Pier	Gust Factors (wind tunnel data)	C_{dyn} Factors * (AS/NZS1170.2:2011 data)
1	1.95	0.85
2	1.95	0.85
3	1.95	0.85
4	1.95	0.85
5	2.00	0.86
6	2.00	0.86
7	2.05	0.88

* note C_{dyn} Factor determined for I_u = 0.1415

The Gust Factors should be used with the wind tunnel data as follows:

$$D_{ULS} = C_{\underset{wt}{\bar{D}}} * G * 0.5 * \rho * \bar{V}^2 * b * \left(\frac{span(a)}{2} + \frac{span(b)}{2}\right) \quad (1)$$

where

$C_{\underset{wt}{\bar{D}}}$ is a Mean Drag Coefficient

$\bar{V}$ is a mean wind speed

and C_{dyn} factors should be used with drag coefficients from AS/NZS1170.2:2011 as follows:

$$D_{ULS} = C_{\underset{AS1170.2}{D}} * C_{dyn} * 0.5 * \rho * \hat{V}^2 * b * \left(\frac{span(a)}{2} + \frac{span(b)}{2}\right) \quad (2)$$

where

$C_{\underset{AS1170.2}{D}}$ is a drag coefficient from AS/NZ1170.2:2011

$\hat{V}$ is a design gust (peak) wind speed

However, although not explicitly stated, the wind tunnel mean drag coefficients could be used using the AS/NZS1170.2:2011 quasi-steady approach as follows:

$$D_{ULS} = C_{\underset{wt}{\bar{D}}} * C_{dyn} * 0.5 * \rho * \hat{V}^2 * b * \left(\frac{span(a)}{2} + \frac{span(b)}{2}\right) \quad (3)$$

Based on the following relationships between mean and gust wind speeds and *G* and C_{dyn} the outcome of the of this analysis for this particular case would result in the same drag load values as follows:

$C_{dyn} = \frac{G}{(1+3.7\ I_u)^2}$, $\hat{V} = \bar{V} * (1 + 3.7\ I_u)$, and substituting into (3)

$$D_{uls} = C_{\underset{wt}{\bar{D}}} * \frac{G}{(1 + 3.7\ I_u)^2} * 0.5 * \rho * \left(\bar{V}\ (1 + 3.7\ I_u)\right)^2 * b * \left(\frac{span(a)}{2} + \frac{span(b)}{2}\right)$$

$$D_{uls} = C_{\underset{wt}{\bar{D}}} * \frac{G}{(1 + 3.7\ I_u)^2} * 0.5 * \rho * \bar{V}^2 * (1 + 3.7\ I_u)^2 * b * \left(\frac{span(a)}{2} + \frac{span(b)}{2}\right)$$

Therefore,

$$D_{uls} = C_{\underset{wt}{D}} * G * 0.5 * \rho * \bar{V}^2 * b * \left(\frac{span(a)}{2} + \frac{span(b)}{2}\right) \quad (4)$$

Equation (4) is the same as Equation (1). Equation (1) would be preferred for the evaluation of the drag wind loads when using the wind tunnel data.

An example of the application of the Gust Factors to the wind tunnel sectional model data is as follows:

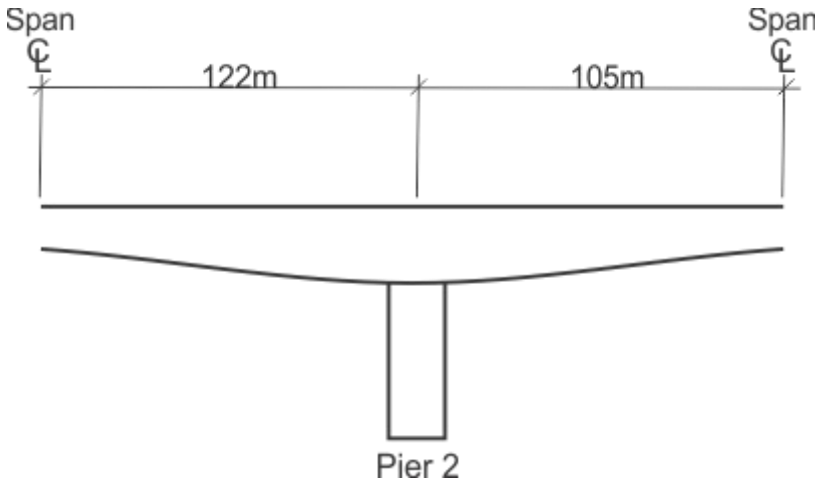

For Span 2 located on the upstream side of the existing AHB.

$$C_{\substack{\bar{D} \\ wt}} = 1.50\ ,\ Gust\ Factor = (G)1.95,\ b = 5.5m$$

From AS1170.2:2011 for TC1.5 and h = 46m (above water) at ULS

$$V_{\substack{R \\ 1000}} = 46\ ms^{-1}$$

$$\hat{V}_{\substack{46 \\ TC1.5 \\ 1000yr}} = 46 * 1.209 = 55.61\ ms^{-1}$$

Mean ULS wind speed

$$\bar{V} = \frac{55.61}{1 + 3.7 * 0.1415}$$

Mean Sectional Drag/unit Length

$$= C_{\substack{\bar{D} \\ wt}} * 0.5 * \rho * \bar{V}^2 * b * (1)$$

$$= 1.5 * 0.5 * 1.2 * 36.5^2 * 5.5 * (1)$$

$$= 6.595\ x\ 10^3\ Nm^{-1}$$

Mean Drag on Pier 2

$$\bar{D} = 6.6\ x\ 10^3 * (122 + 105)$$

$$= 1.50\ x\ 10^6\ N$$

Design ULS Drag on Pier 2

$$D_{ULS} = G * \overline{D}$$
$$= 1.95 * 1.50\ x\ 10^6$$
$$= 2.92\ x\ 10^6\ N$$

4 CONCLUSIONS

Wind tunnel tests have been carried out on a sectional model of the proposed Auckland Harbour Bridge Cycleway in turbulent flow to determine the sectional mean force and moment characteristics and aerodynamic damping properties over a range of angles of attack between -10 degrees and +15 degrees. Due to the interaction with the existing Auckland Harbour Bridge (AHB), the rigid sectional model was tested in six Section Studies, outlined as follows:

- Section Study 1 – Span 2 located upstream of the existing AHB
- Section Study 2 – Span 2 located downstream of the existing AHB
- Section Study 3 – Span 4 located upstream of the existing AHB
- Section Study 4 – Span 4 located downstream of the existing AHB
- Section Study 5 – Viewing Platform located upstream of the existing AHB
- Section Study 6 – Viewing Platform located downstream of the existing AHB

The proposed design was found to suffer from aerodynamic instability, so further investigations were commissioned and performed to investigate aerodynamic strategies to achieve stability. In addition, modifications were made to the structural design of the Cycleway to increase the modal frequencies. BECA have opted for strategies that include aerodynamic modifications and damping to achieve stability for wind speeds up to and just above ULS. BECA have indicated they will ensure a minimum damping of 5% of critical (structural + damper). The mean force and moment coefficients for all Cycleway Section Studies have been determined and presented for this modified design. The aerodynamic damping for Section Studies 1 to 4 have been determined and presented for the modified design.

For mean force and moment characteristics, Section Studies with the Cycleway upstream of the existing AHB structure were found to be most critical. The data show that there is little significant difference in the mean force and moment coefficients, between Section Studies 1 and 3. The trend of the Lift Coefficients, C_L, in these Section Studies show a generally positive lift slope across the range of angles of attack tested. Variation in Drag Coefficients, C_D, with changing angle of attack is shown to fall between 1.6 and 0.8 for both

Section Studies 1 and 3. Similarly, the Moment Coefficients, C_M, in these two Section Studies have been shown to be positive for all angles of attack, ranging from 0.75 to 0.35.

The data show that the mean force and moment coefficients for the Viewing Platform are more critical for Section Study 5. The Lift Coefficients, C_L, are shown to exhibit a positive lift slope across the range of angles tested. The mean Drag Coefficients, C_D, are shown to range from 2.6 to 1.8. The mean Moment Coefficients, C_M, show a decreasing trend as the angle of attack moves away from 0 degrees, ranging between 1 to 1.55.

The lift aerodynamic damping of the proposed AHB Cycleway has been determined and presented for all angles of attack and range of Reduced Velocities including Serviceability Limit State (SLS) and Ultimate Limit State (ULS). This has been shown to be negative for all angles of attack for both Section Studies, to reach a highest negative aerodynamic damping of -4.5%.

The Gust Factors and C_{dyn} Factors have been provided to account for the correlation of the drag loads for each pier.

It is recommended that the full aeroelastic bridge wind tunnel model study be undertaken to assess the aerodynamic performance of the Cycleway.

MEL CONSULTANTS

March 2020

FIGURES

Figure 1: Photograph of the proposed Auckland Harbour Bridge Cycleway sectional wind tunnel model in Section Study 1 installed in the Sectional Testing area within the MEL Consultants 400kW Boundary Layer Wind Tunnel

Figure 2: Photograph of the modified Auckland Harbour Bridge Cycleway sectional wind tunnel model in Section Study 2 installed in the Sectional Testing area within the MEL Consultants 400kW Boundary Layer Wind Tunnel

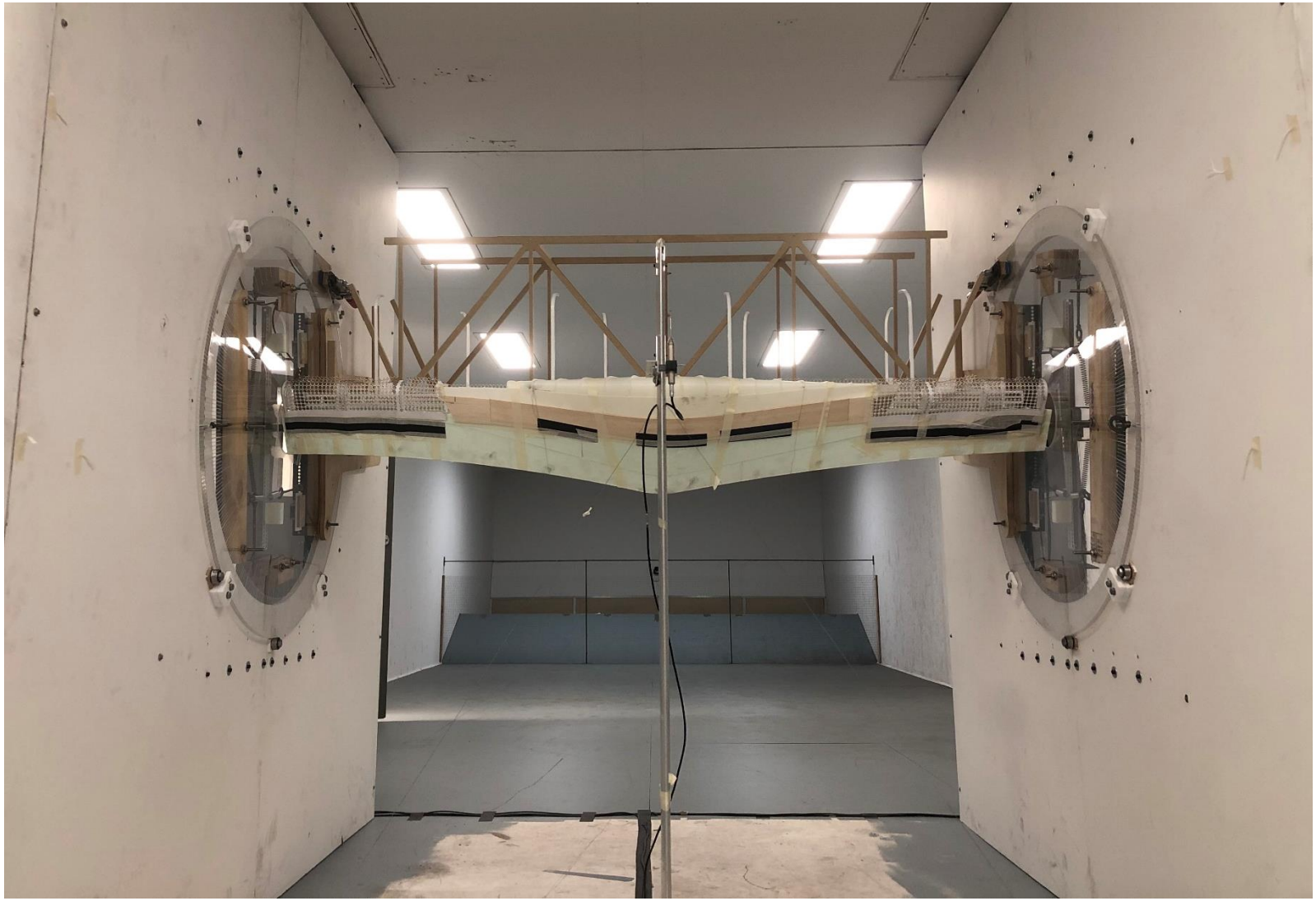

Figure 3: Photograph showing the contour of the Viewing Platform of the modified Auckland Harbour Bridge Cycleway sectional wind tunnel model in Section Study 5.

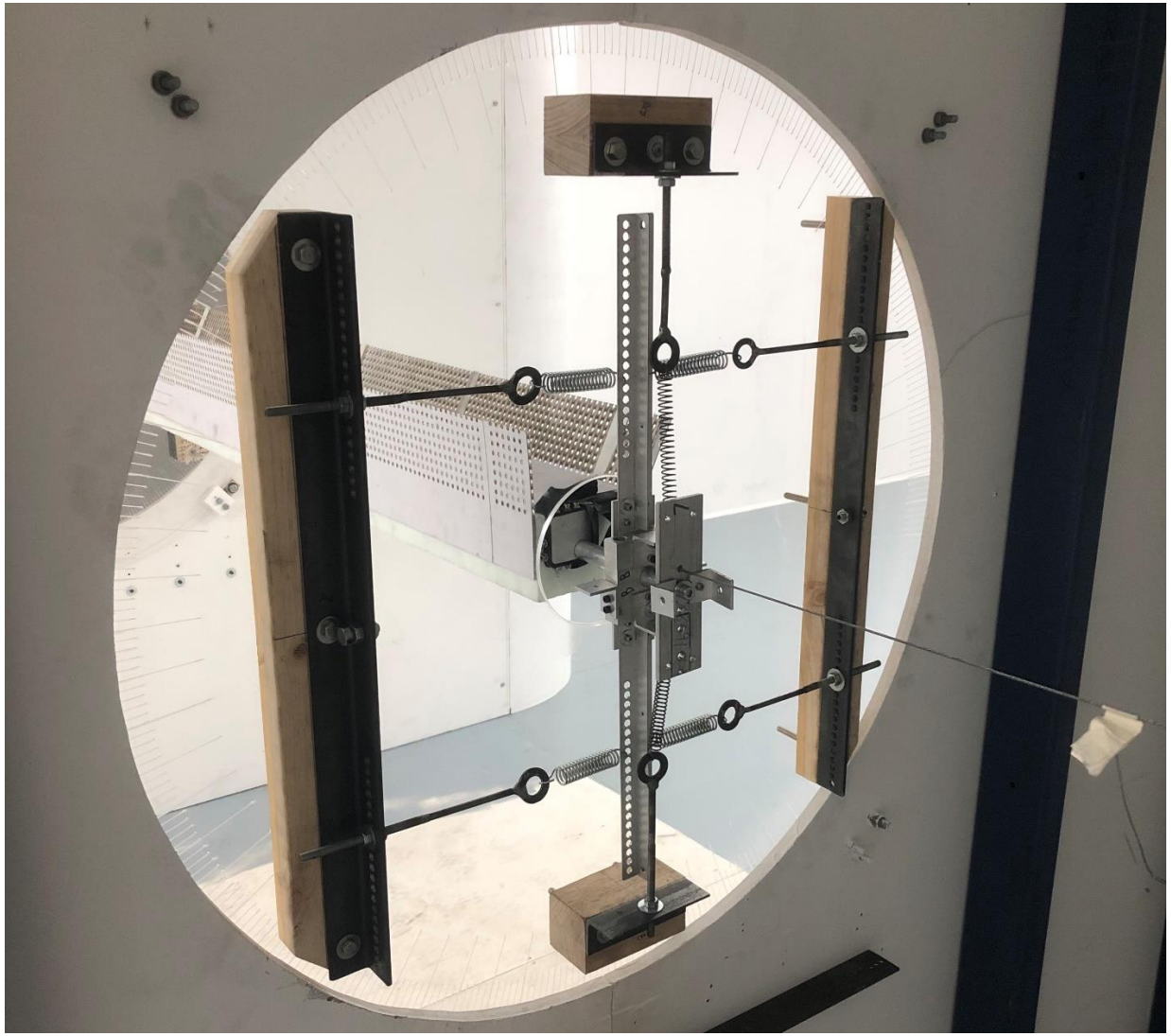

Figure 4: Photograph of the experimental setup for basic mean force and moment coefficients as installed in the Sectional Testing area within the MEL Consultants 400kW Boundary Layer Wind Tunnel.

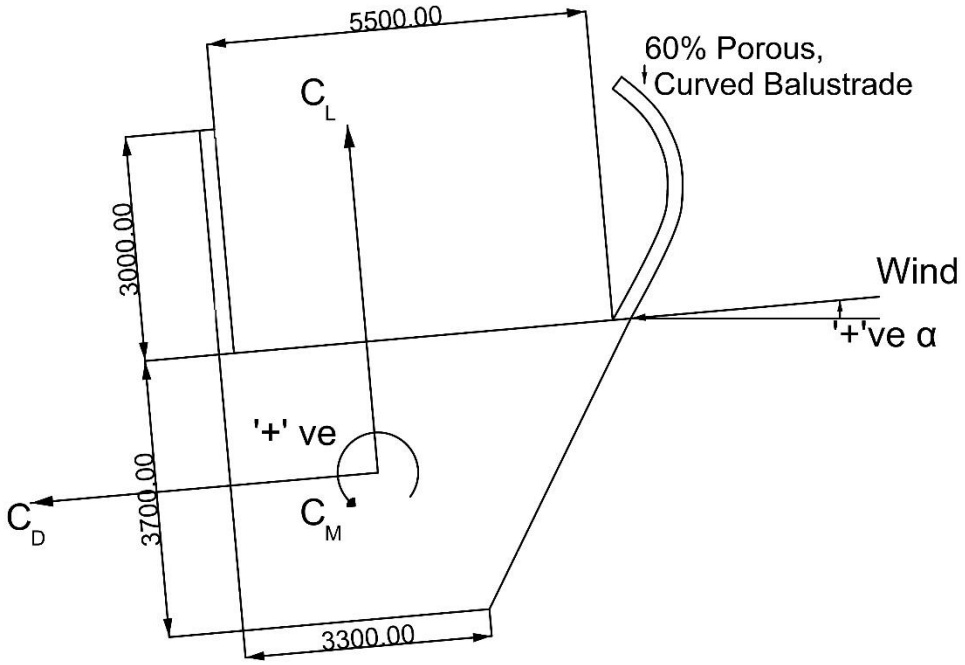

AHB Cycleway Span 2 - Modified Design and Axis Notation

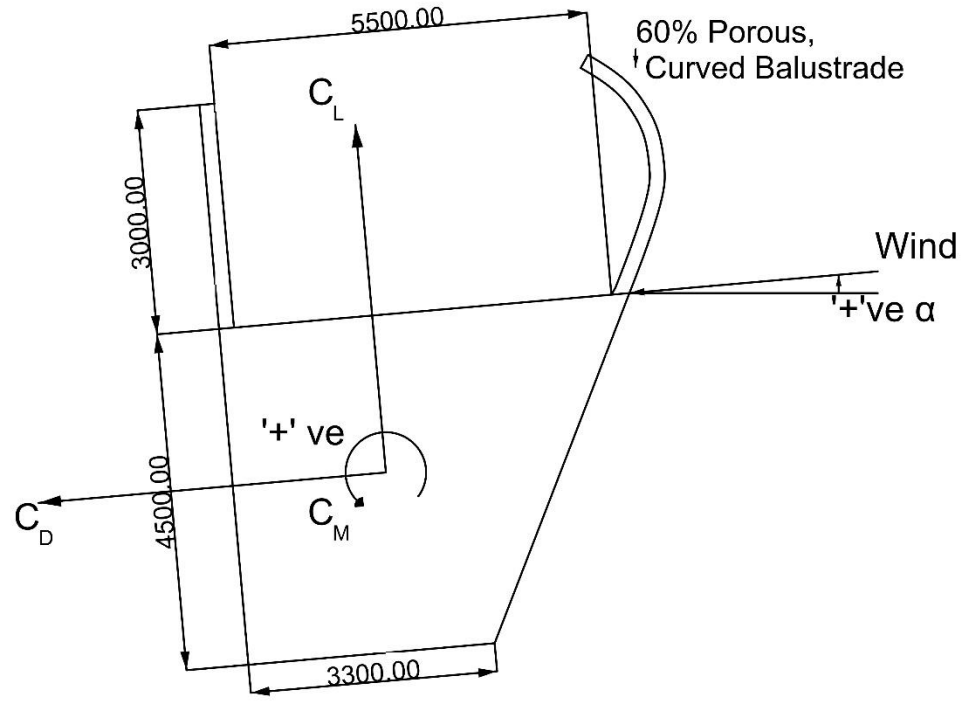

AHB Cycleway Span 4 - Modified Design and Axis Notation

Figure 5: Schematic view of the cross-section of Spans 2 and 4 of the Auckland Harbour Bridge Cycleway as tested, indicating the co-ordinate system used.

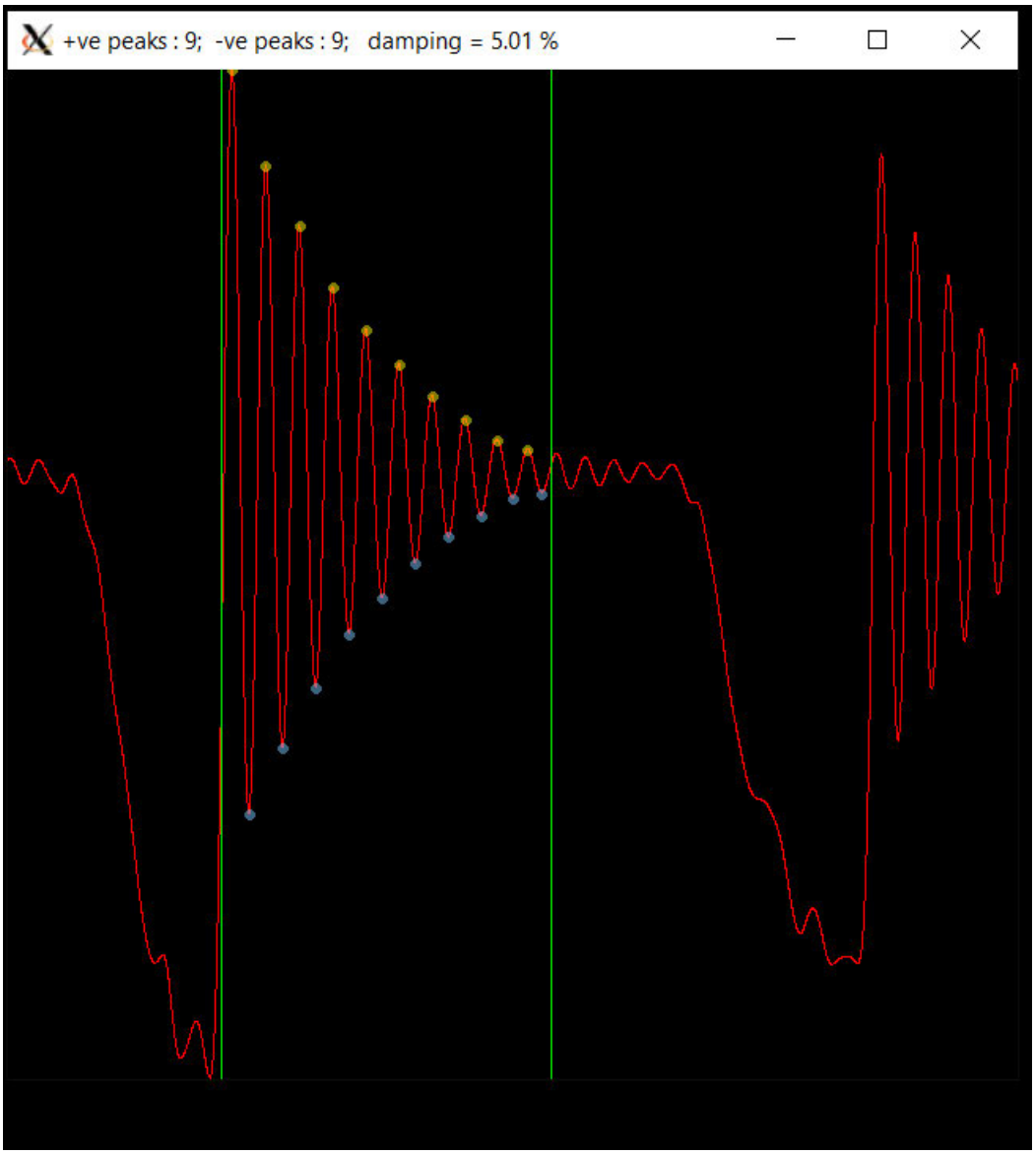

Figure 6: Damping trace from Sectional Model Study

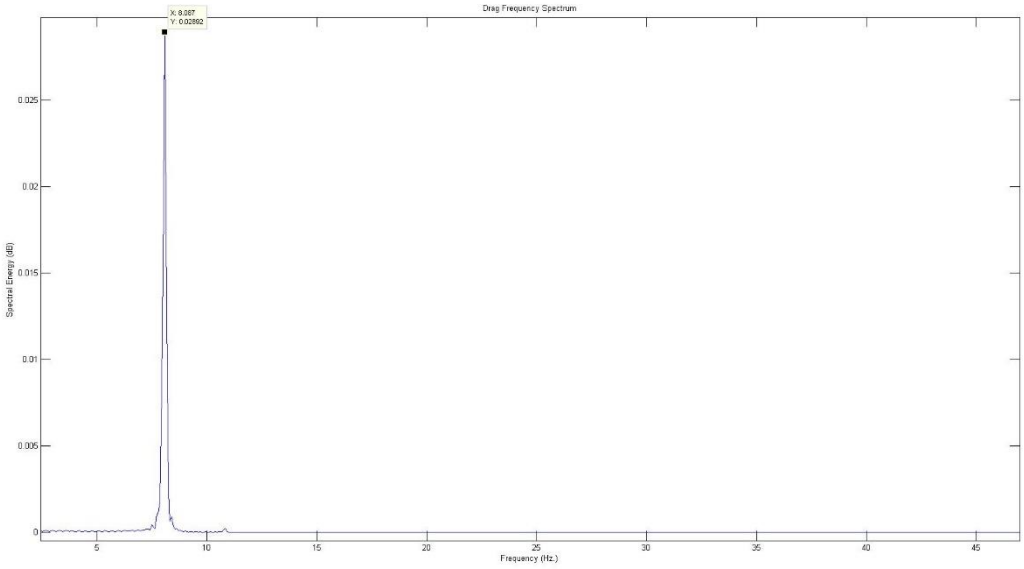

Figure 7: Lateral (drag) sectional model frequency

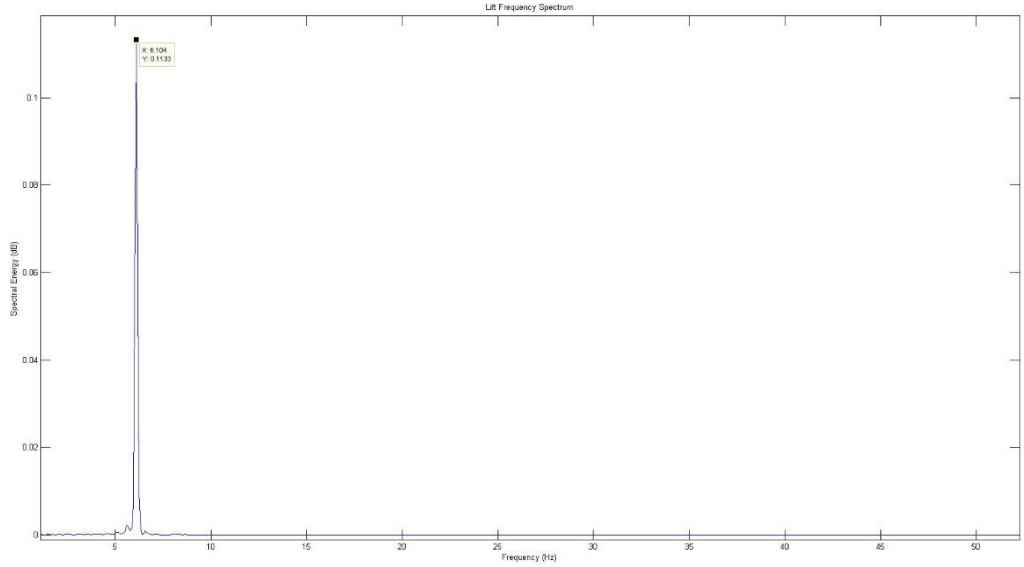

Figure 8: Vertical (lift) sectional model frequency

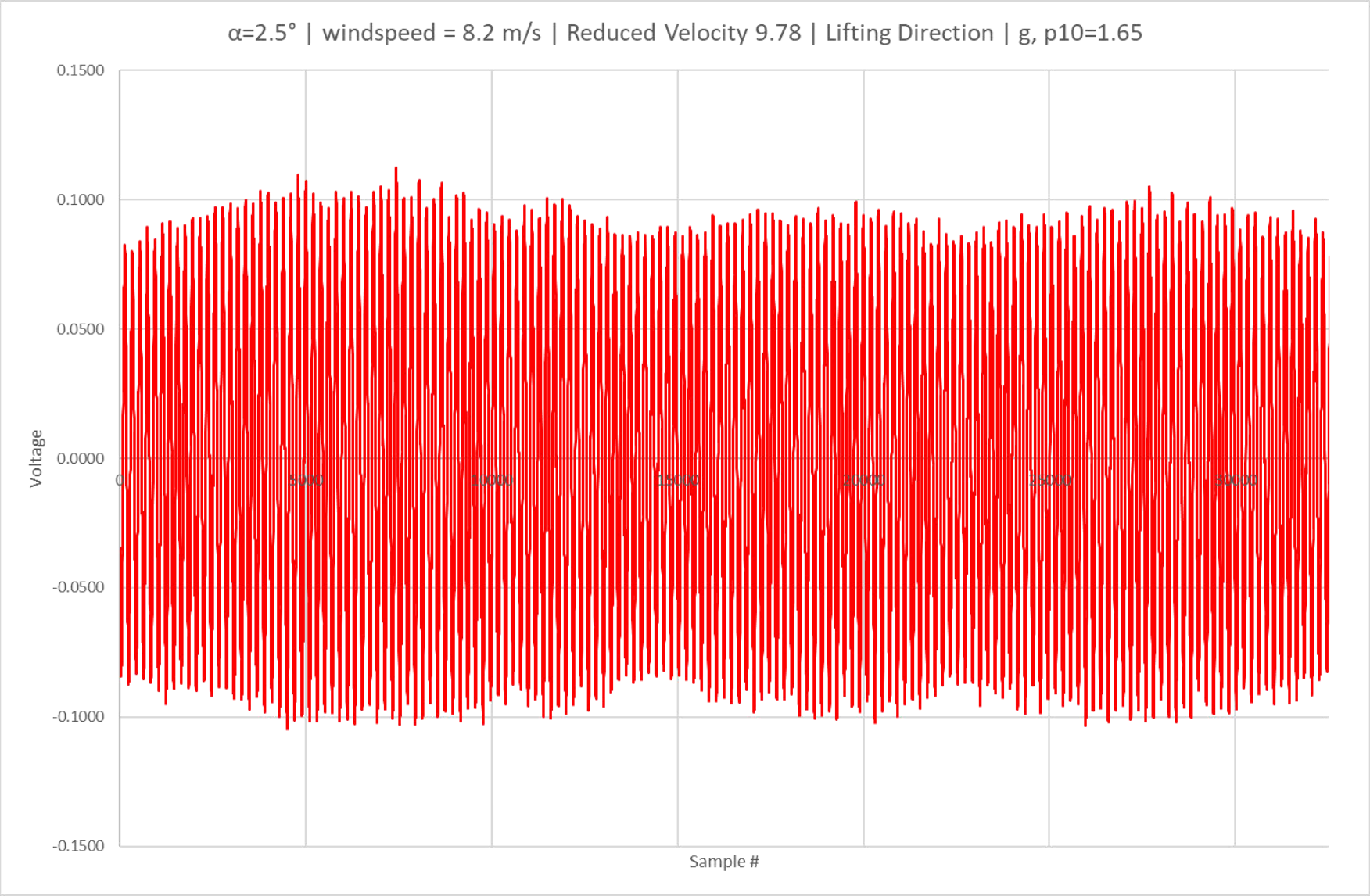

Figure 9: A displacement response time series of the proposed, unstable, Auckland Harbour Bridge Cycleway.

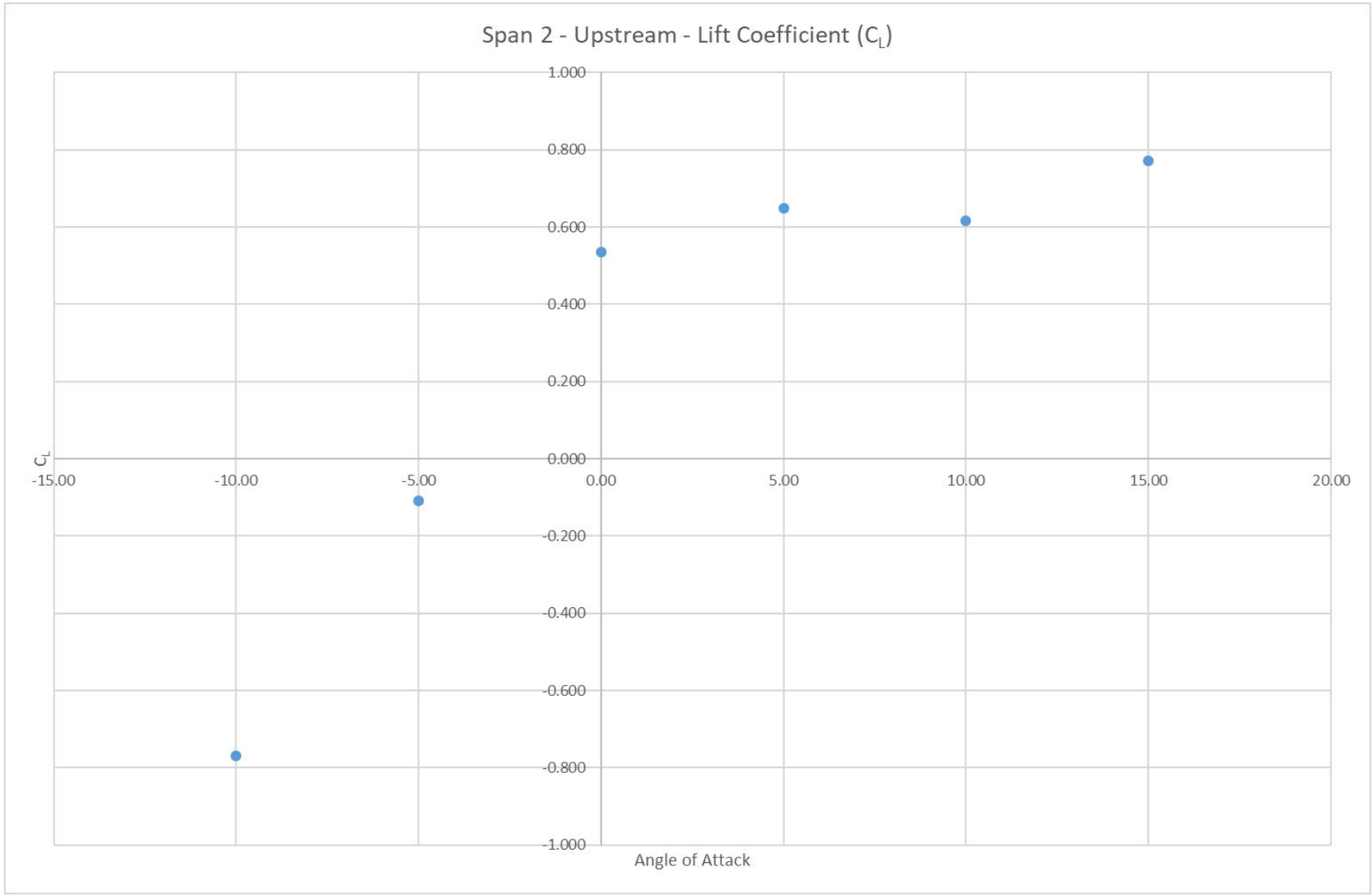

Figure 10: C_L for Section Study 1 of the modified Auckland Harbour Bridge Cycleway as a function of angle of attack.

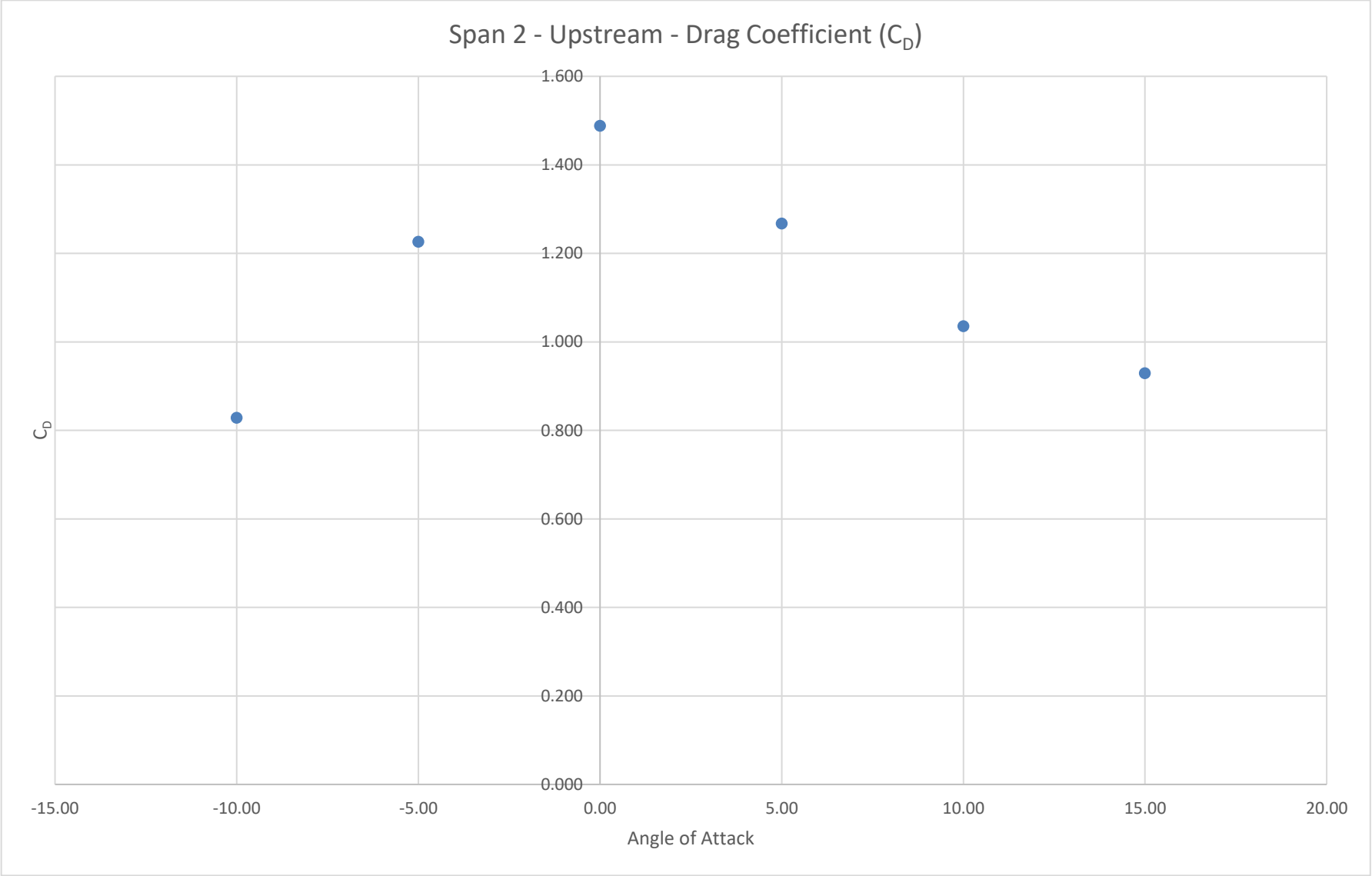

Figure 11: C_D for Section Study 1 of the modified Auckland Harbour Bridge Cycleway as a function of angle of attack.

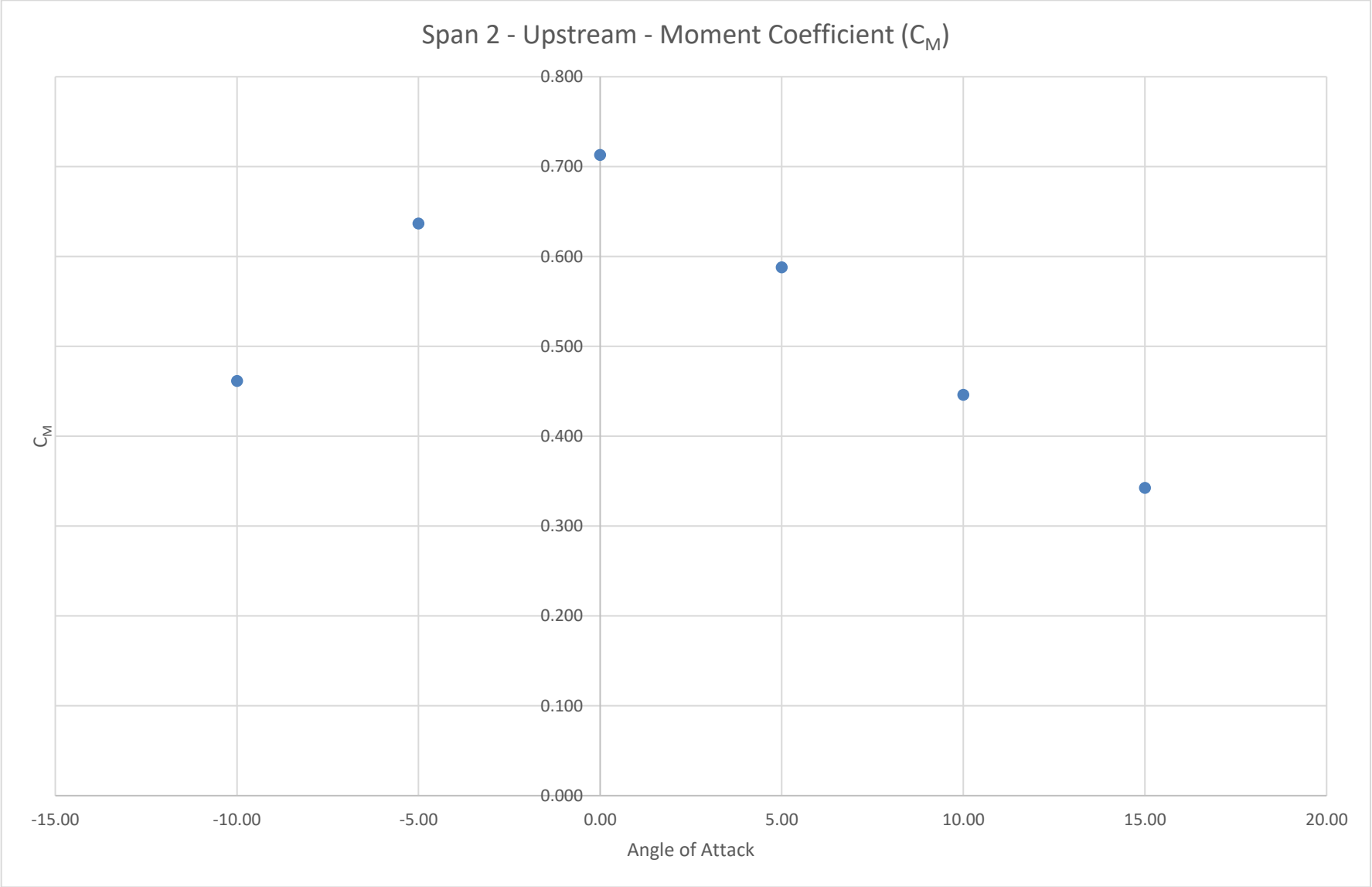

Figure 12: C_M for Section Study 1 of the modified Auckland Harbour Bridge Cycleway as a function of angle of attack.

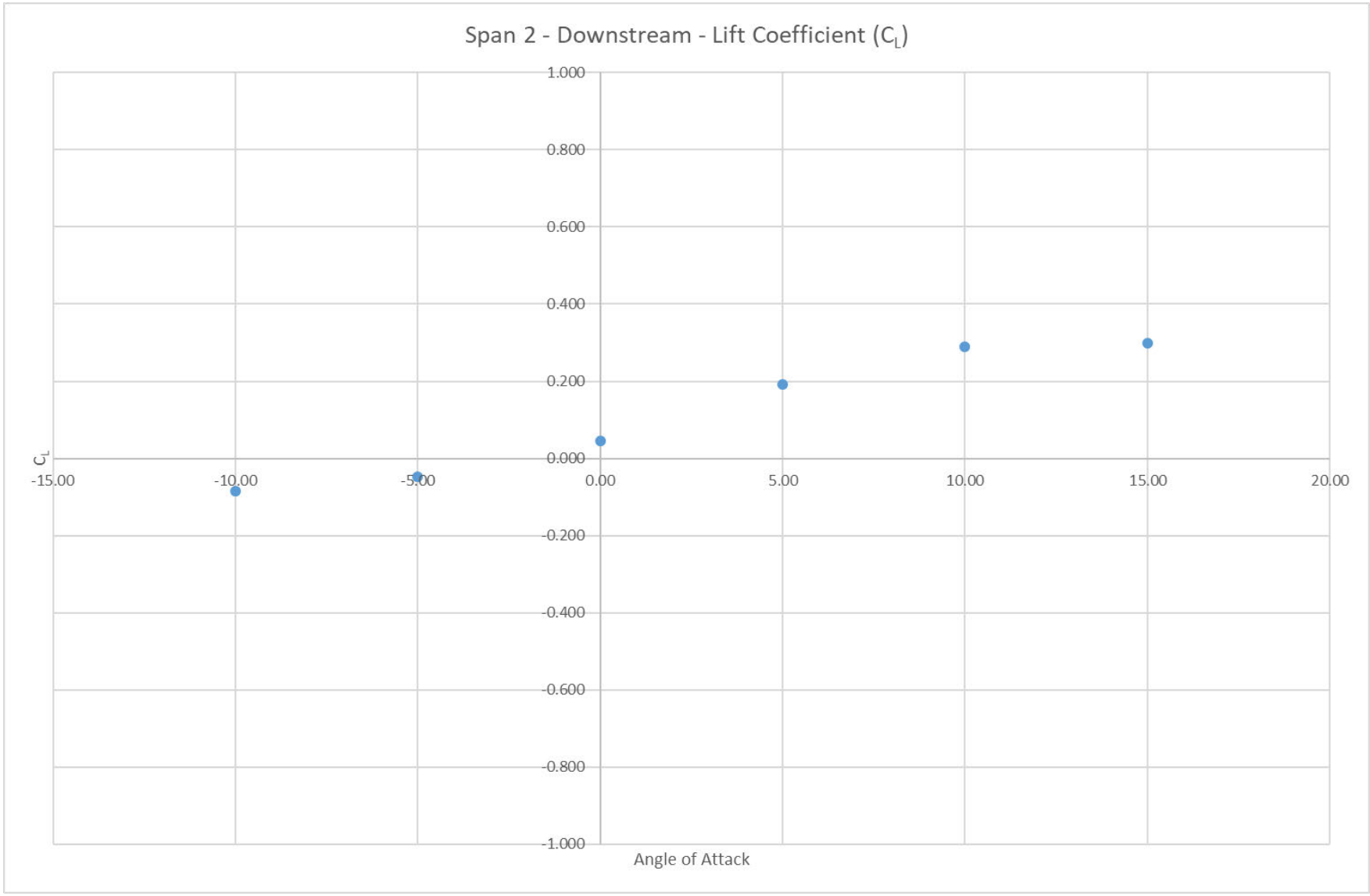

Figure 13: C_L for Section Study 2 of the modified Auckland Harbour Bridge Cycleway as a function of angle of attack.

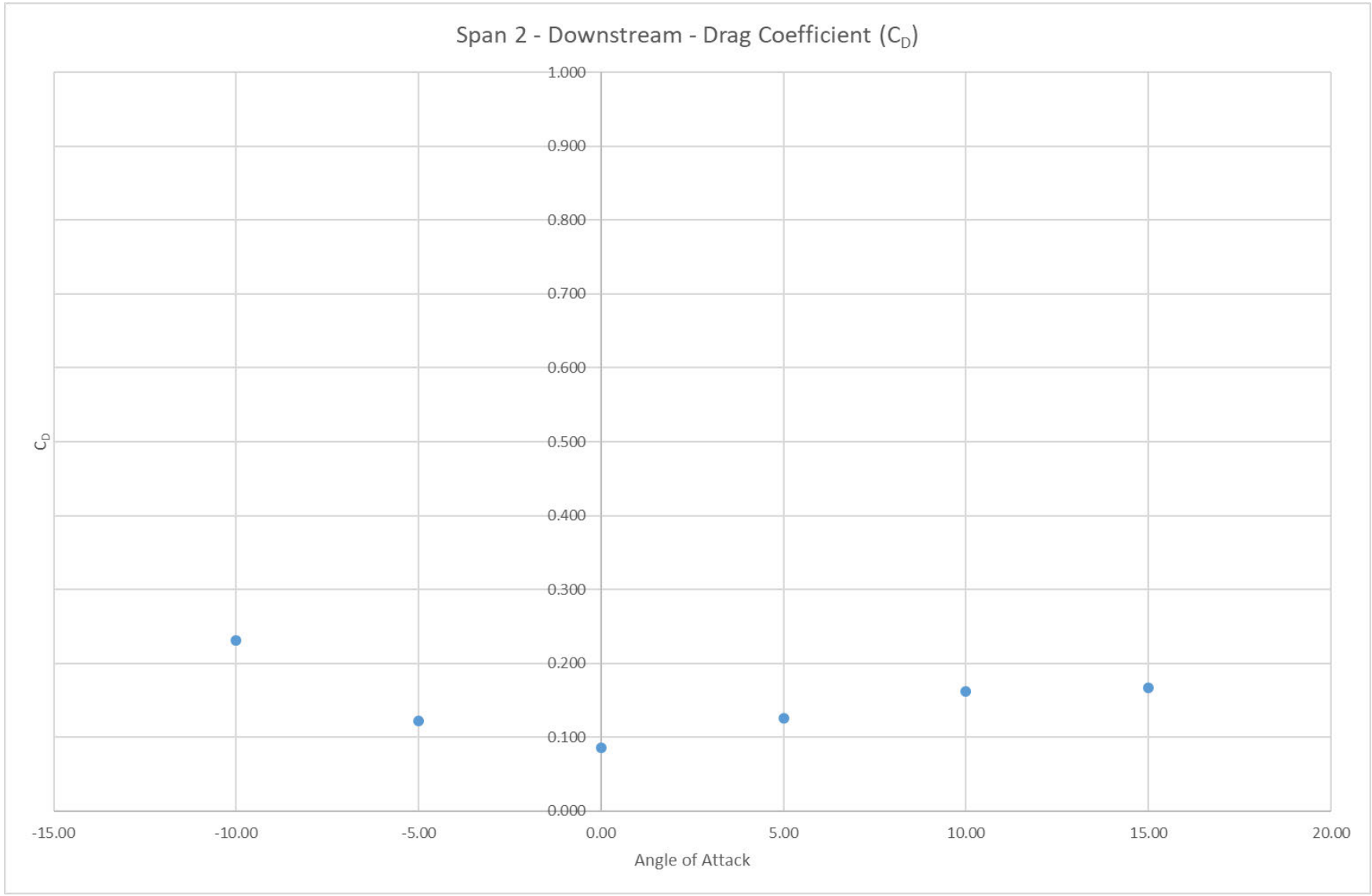

Figure 14: C_D for Section Study 2 of the modified Auckland Harbour Bridge Cycleway as a function of angle of attack.

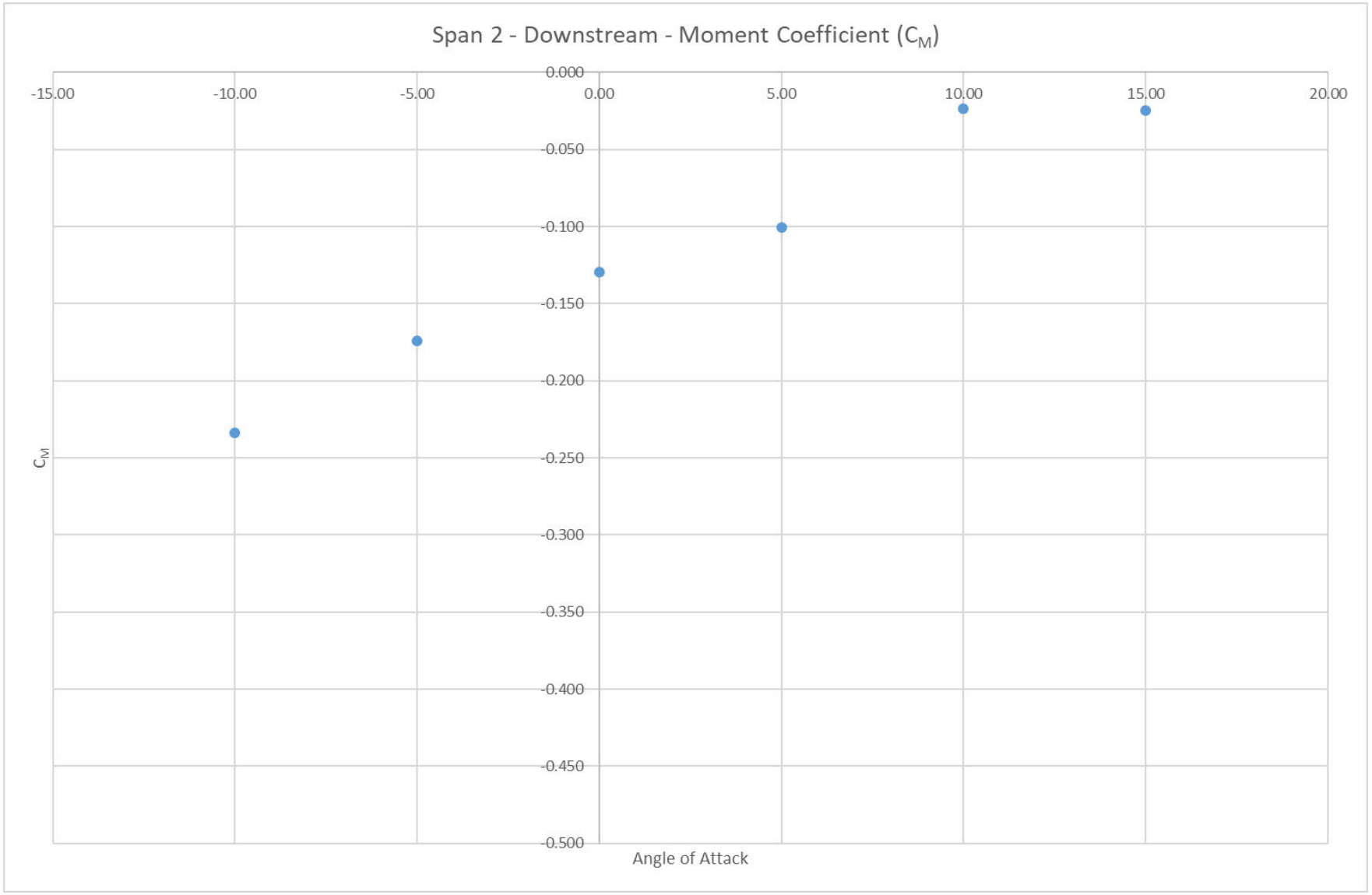

Figure 15: C_M for Section Study 2 of the modified Auckland Harbour Bridge Cycleway as a function of angle of attack.

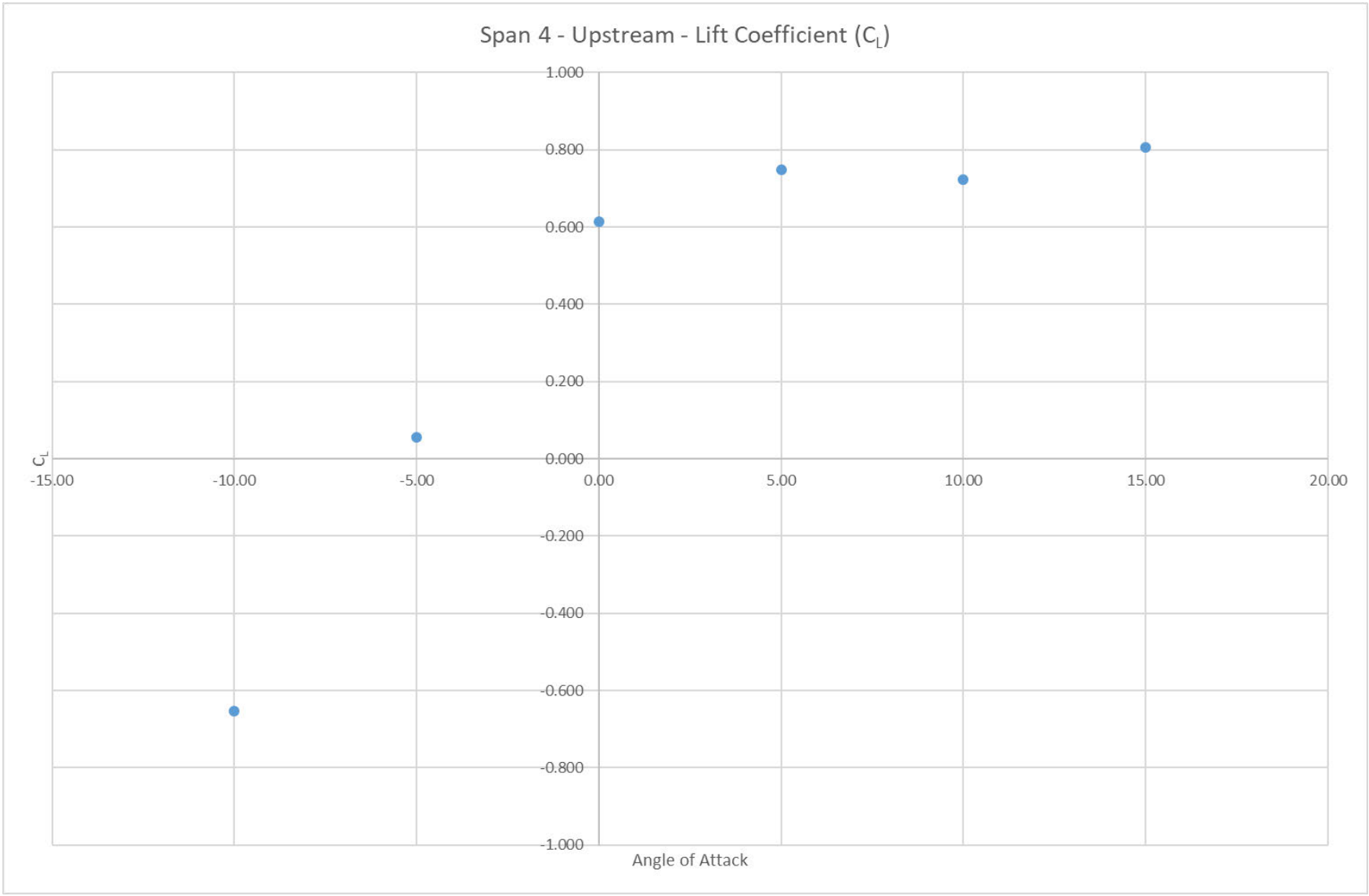

Figure 16: C_L for Section Study 3 of the modified Auckland Harbour Bridge Cycleway as a function of angle of attack.

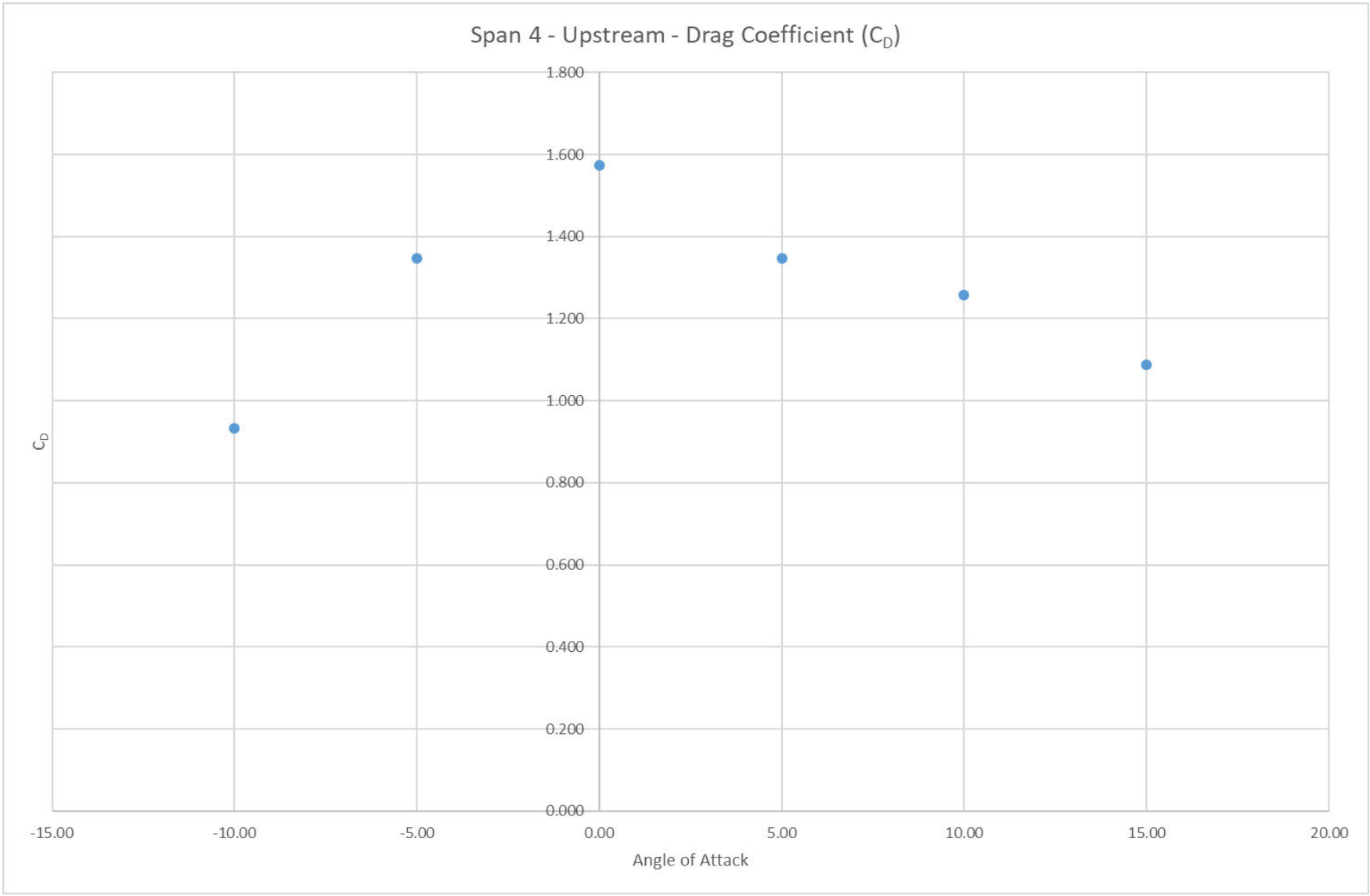

Figure 17: C_D for Section Study 3 of the modified Auckland Harbour Bridge Cycleway as a function of angle of attack.

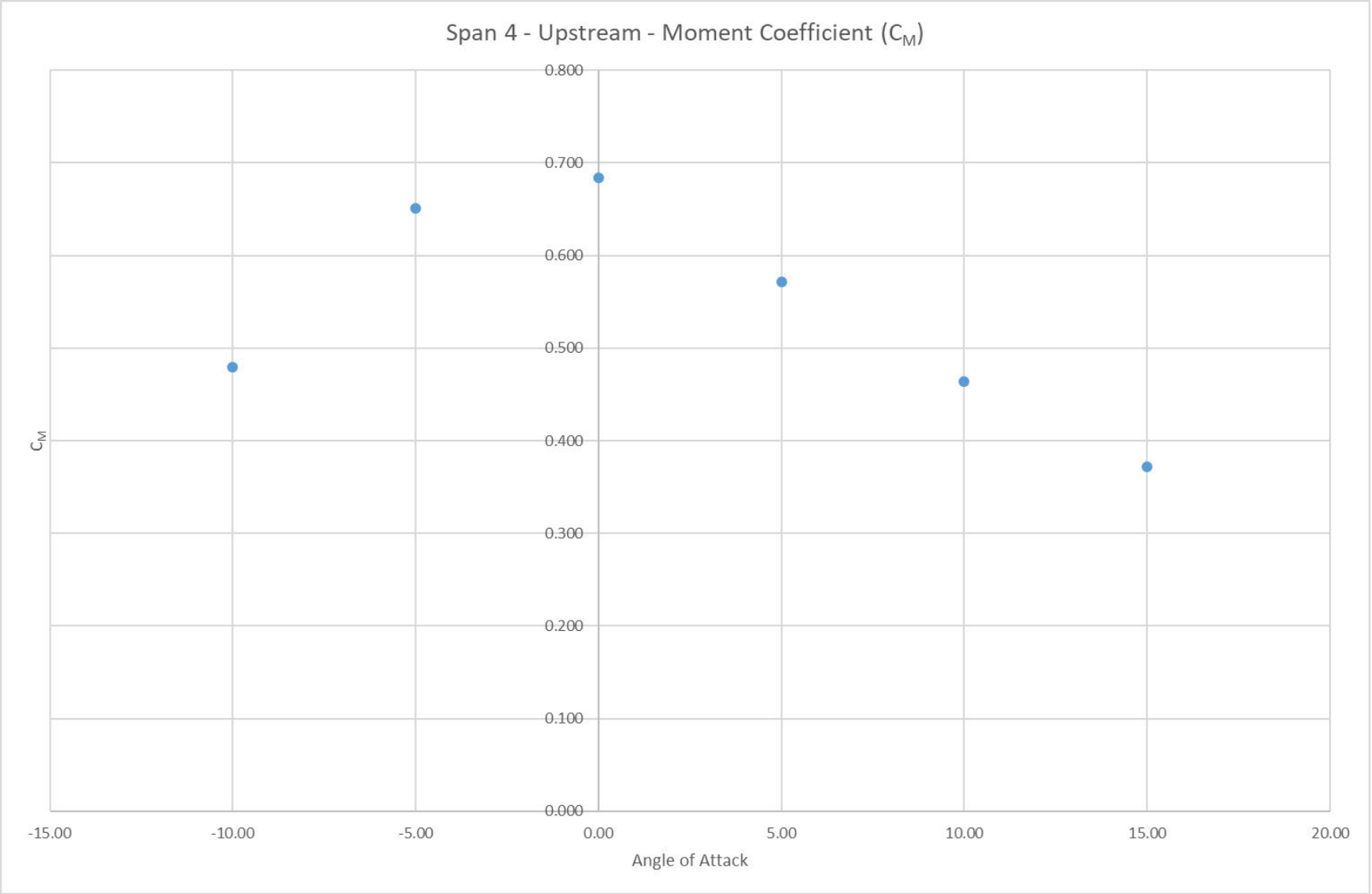

Figure 18: C_M for Section Study 3 of the modified Auckland Harbour Bridge Cycleway as a function of angle of attack.

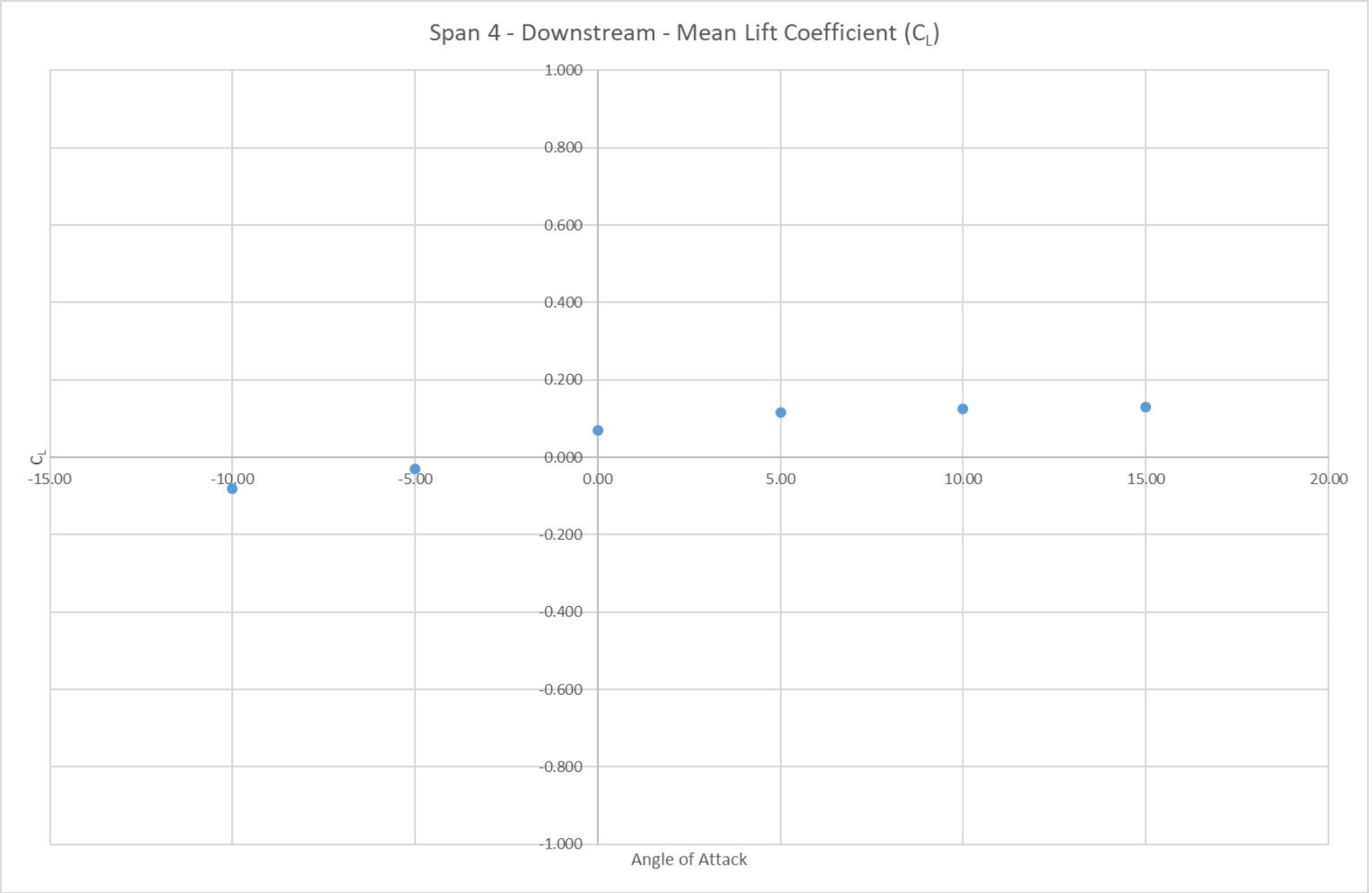

Figure 19: C_L for Section Study 4 of the modified Auckland Harbour Bridge Cycleway as a function of angle of attack.

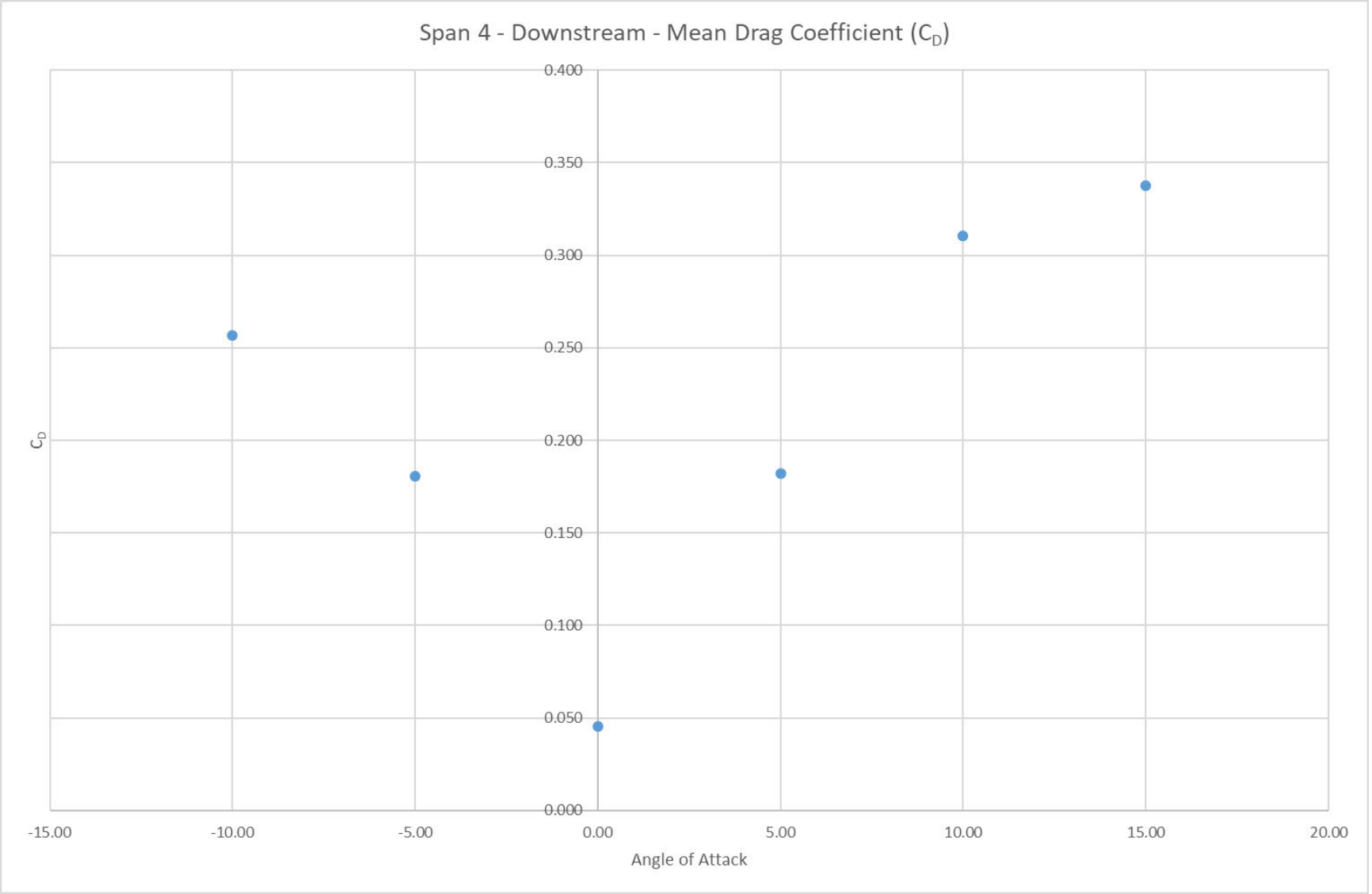

Figure 20: C_D for Section Study 4 of the modified Auckland Harbour Bridge Cycleway as a function of angle of attack.

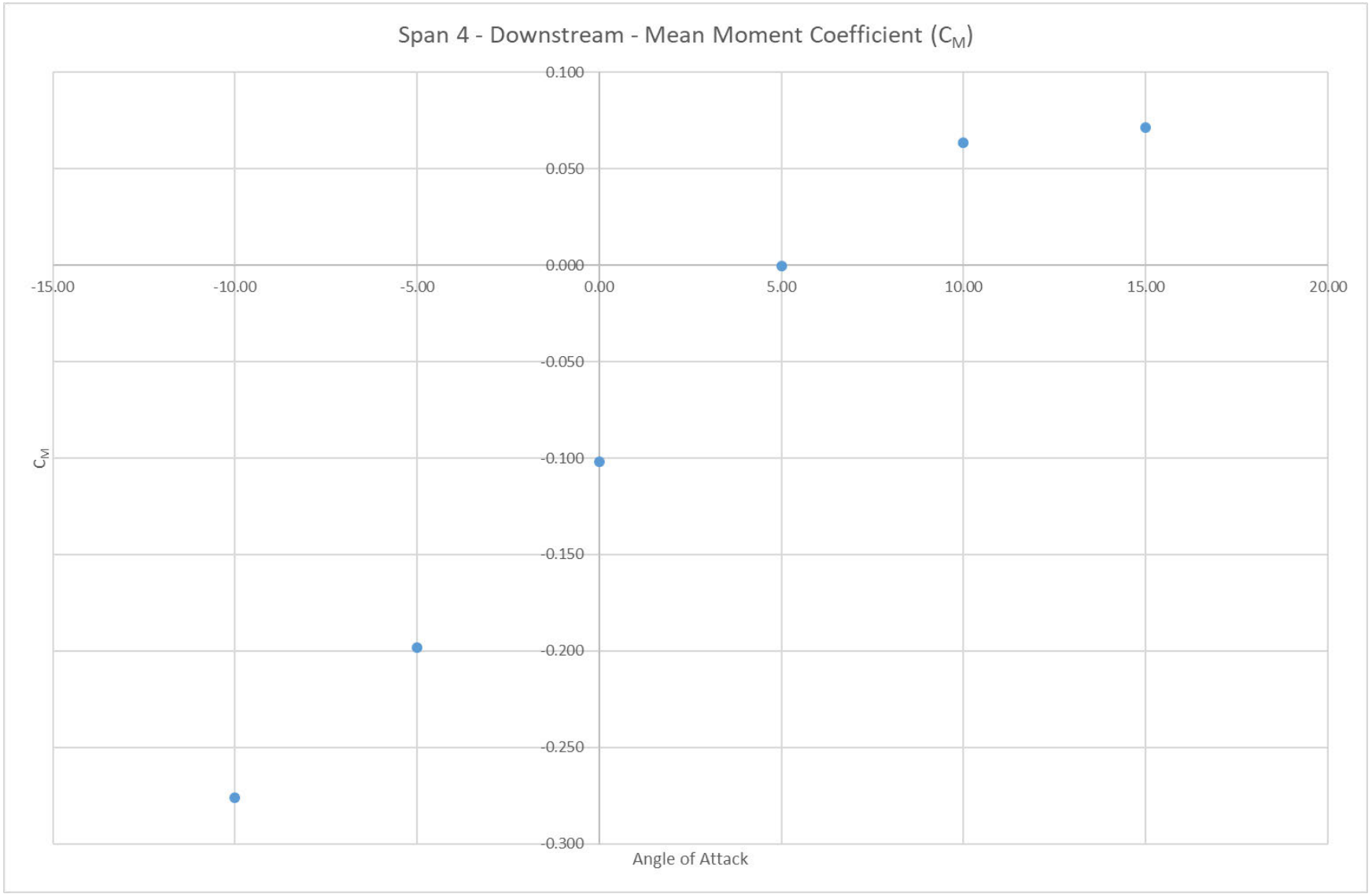

Figure 21: C_M for Section Study 4 of the modified Auckland Harbour Bridge Cycleway as a function of angle of attack.

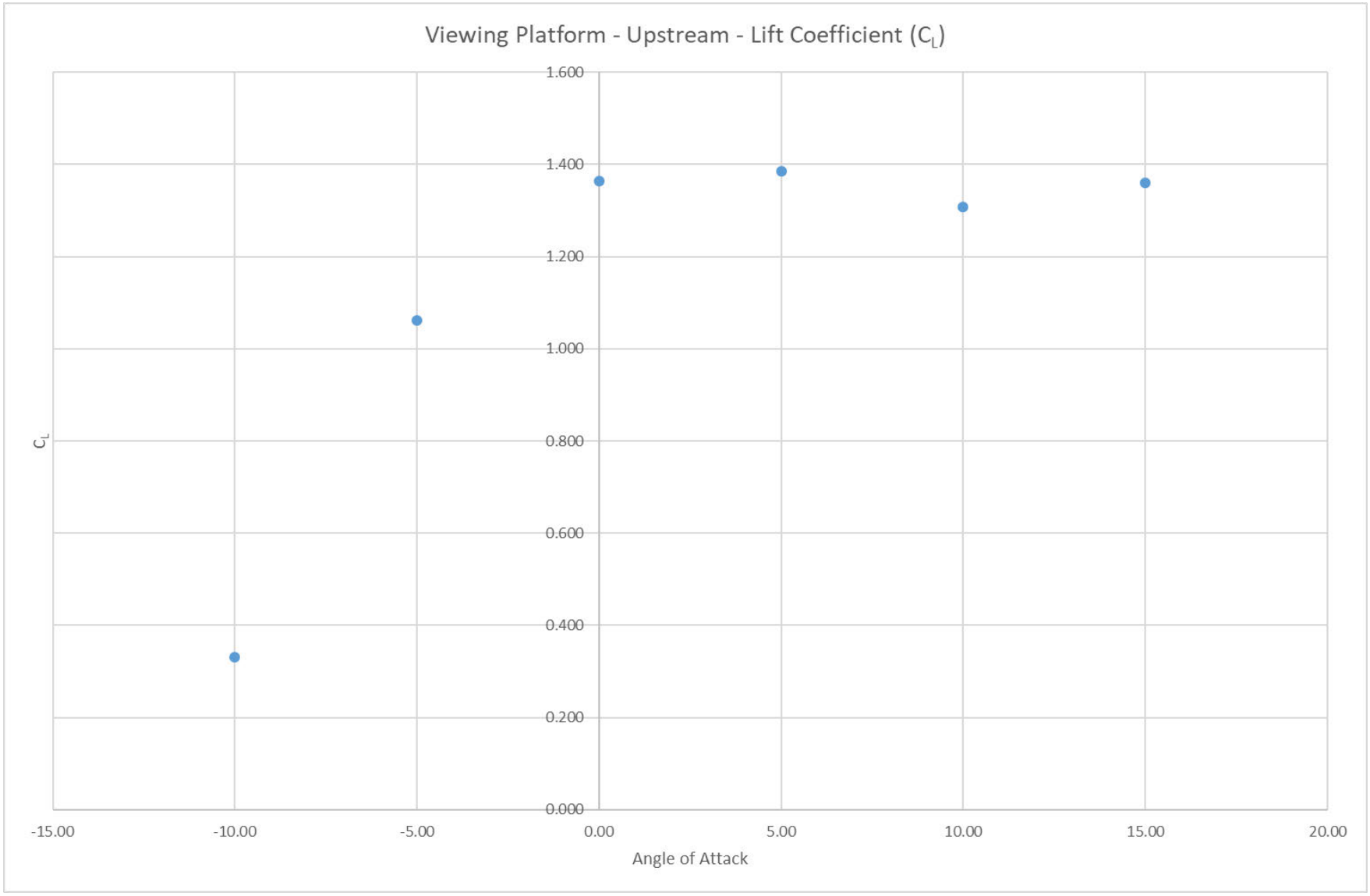

Figure 22: C_L for Section Study 5 of the modified Auckland Harbour Bridge Cycleway as a function of angle of attack.

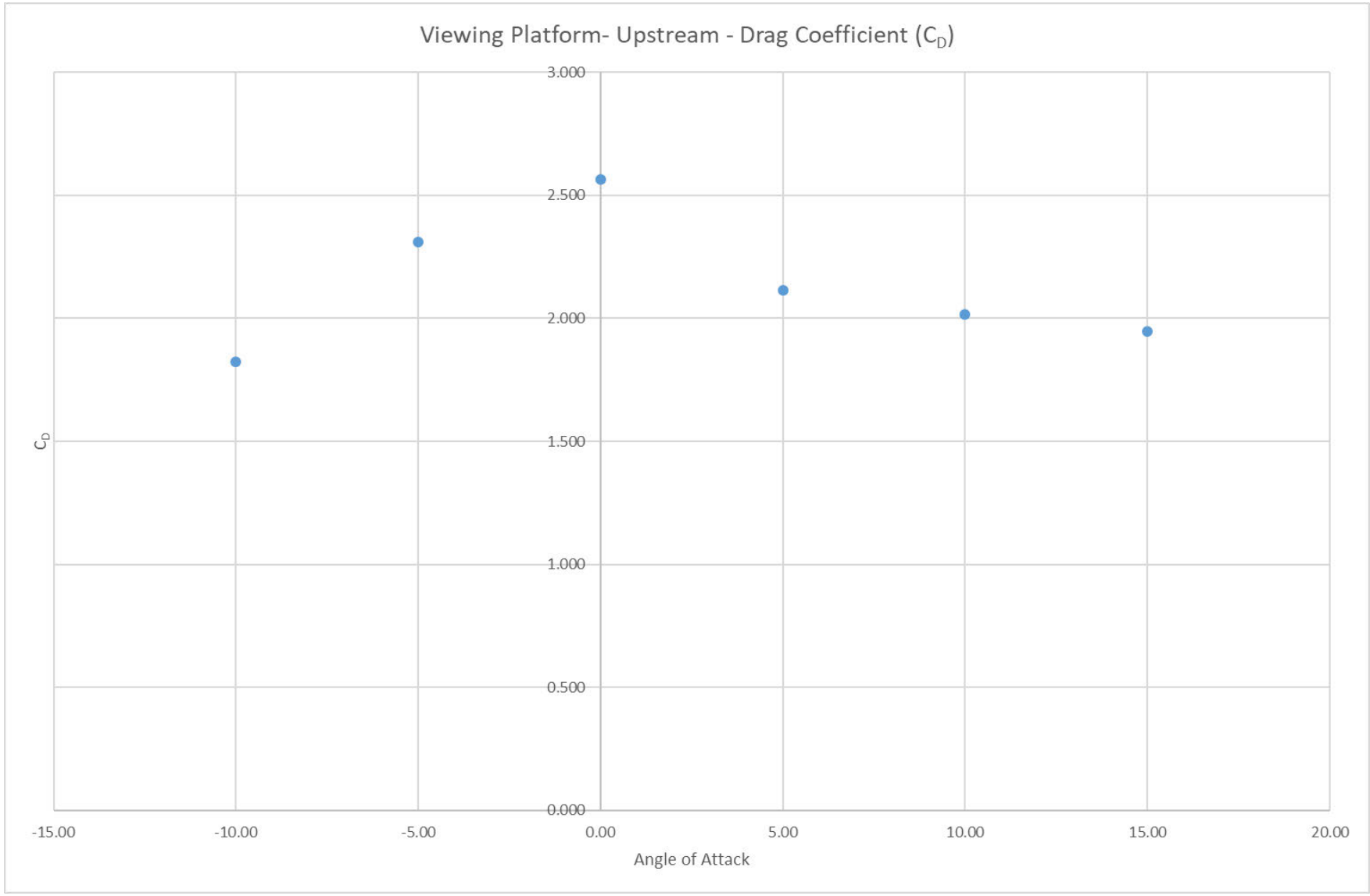

Figure 23: C_D for Section Study 5 of the modified Auckland Harbour Bridge Cycleway as a function of angle of attack.

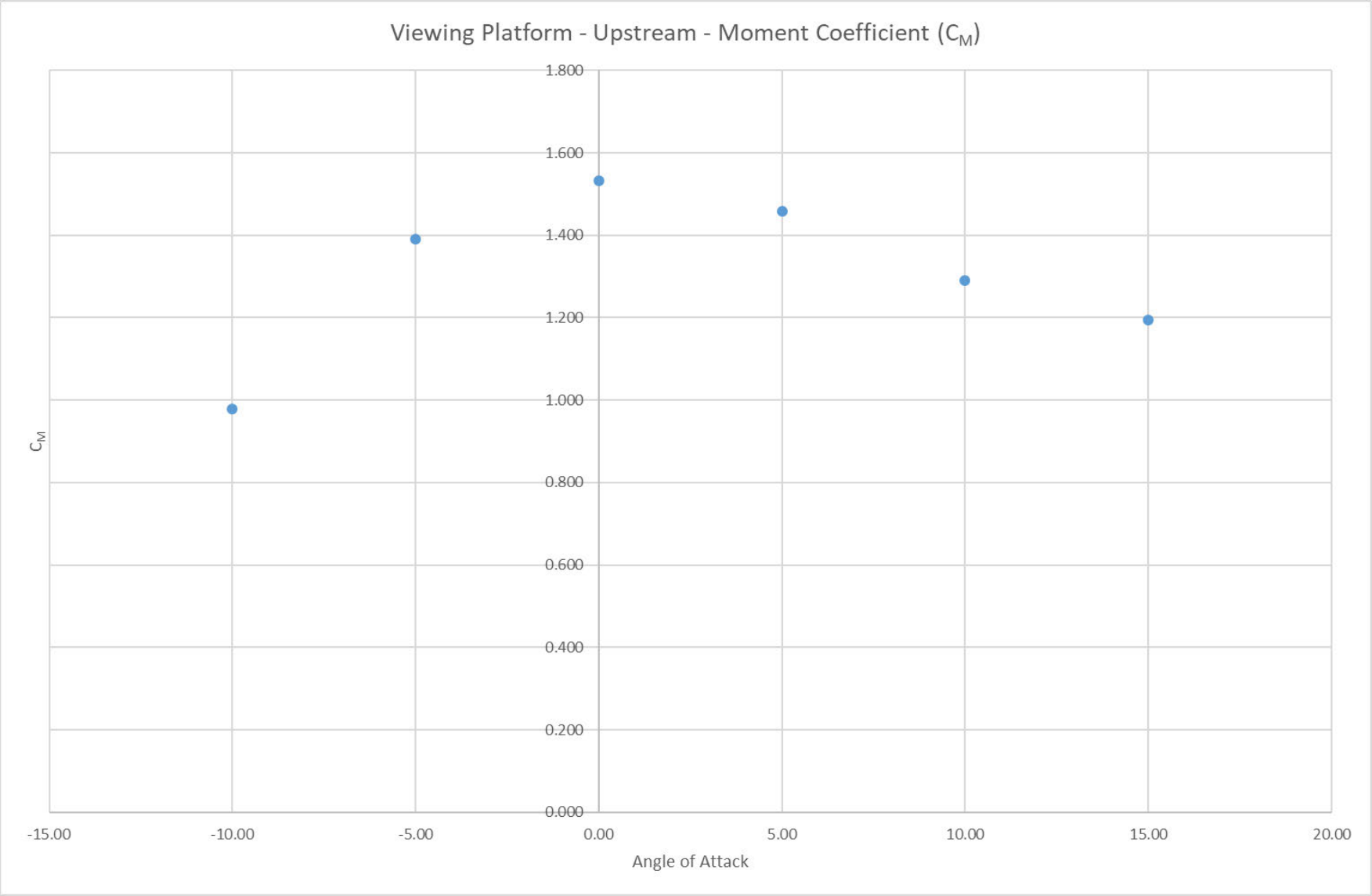

Figure 24: C_M for Section Study 5 of the modified Auckland Harbour Bridge Cycleway as a function of angle of attack.

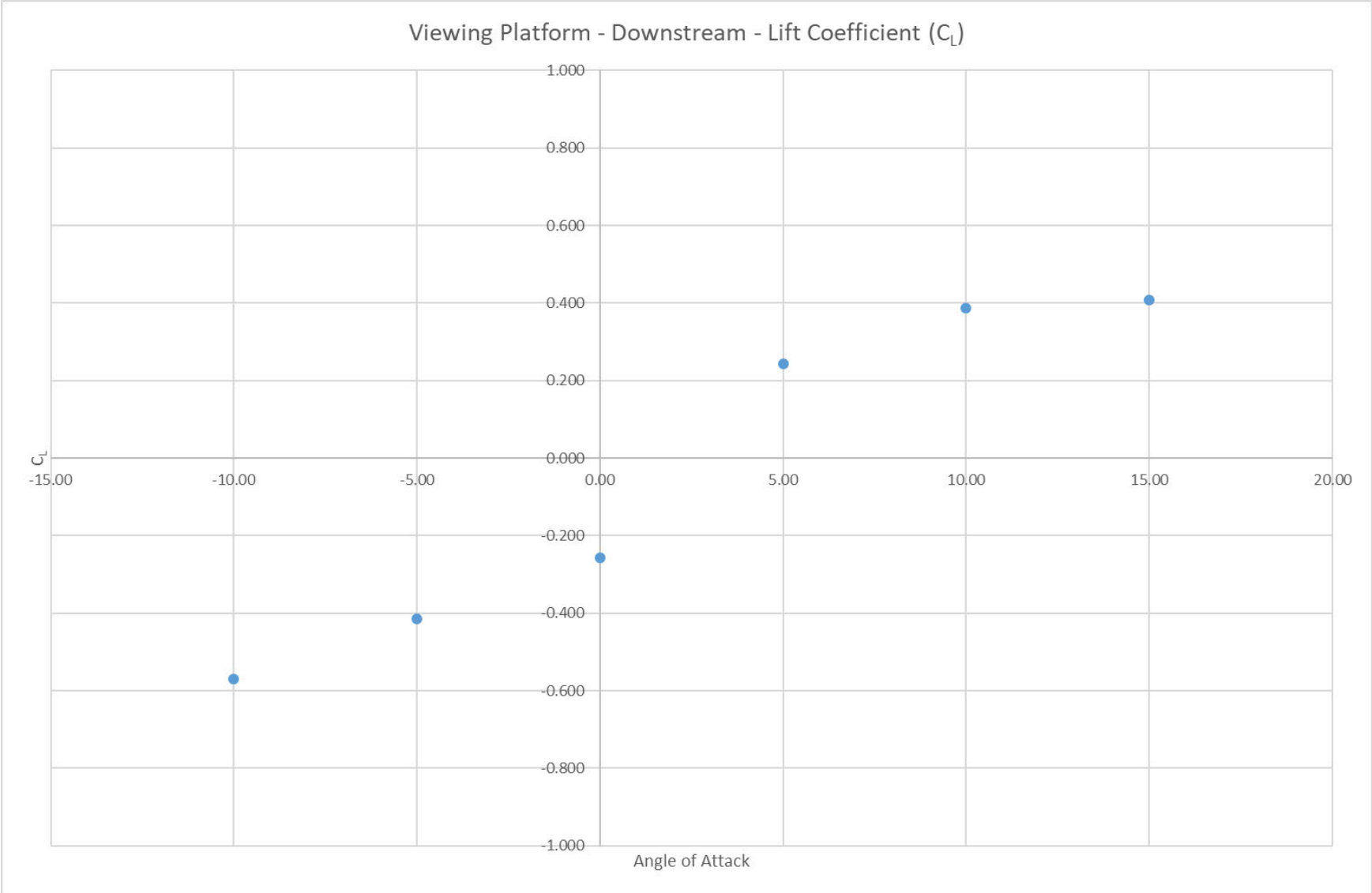

Figure 25: C_L for Section Study 6 of the modified Auckland Harbour Bridge Cycleway as a function of angle of attack.

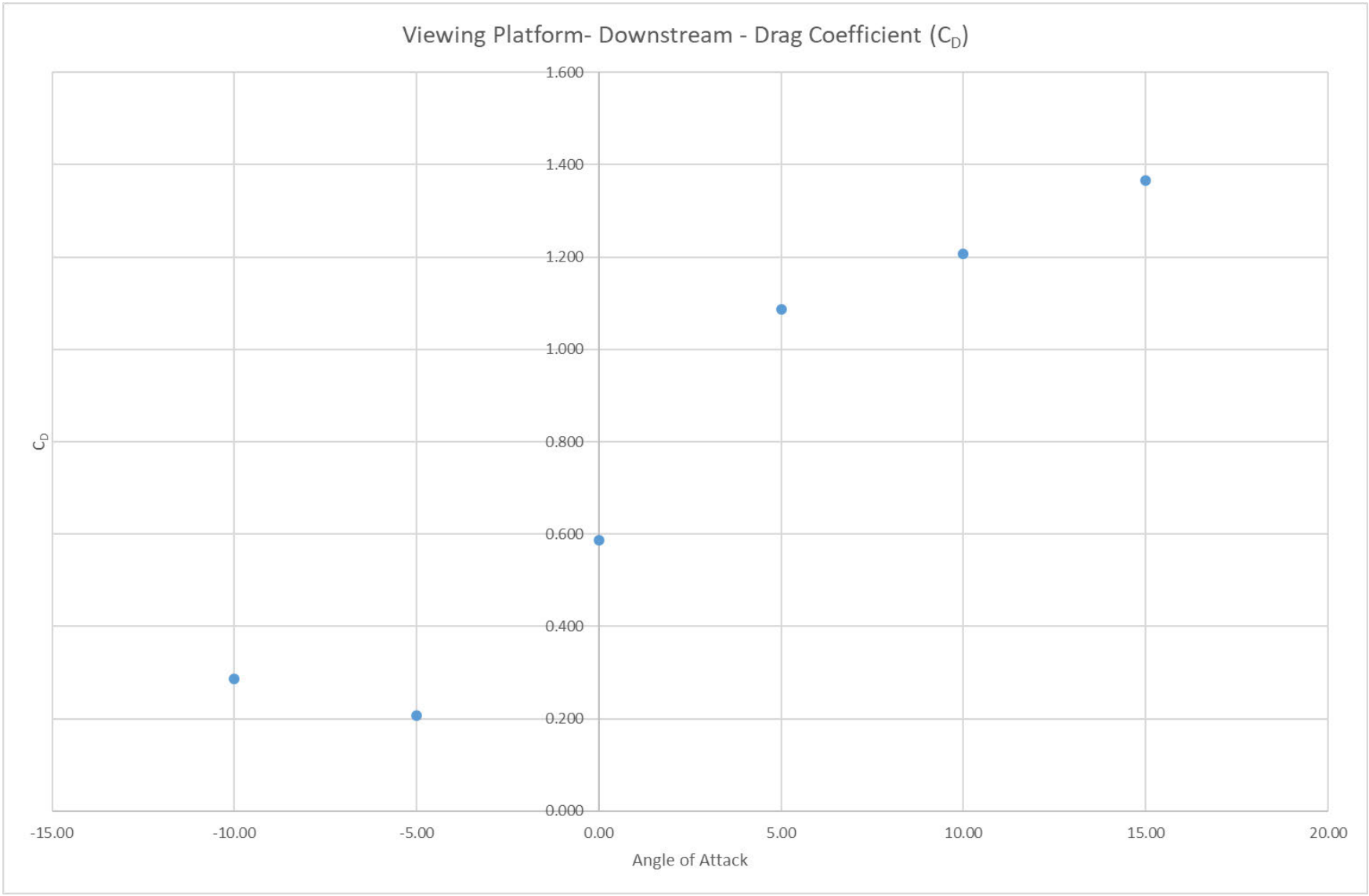

Figure 26: C_D for Section Study 6 of the modified Auckland Harbour Bridge Cycleway as a function of angle of attack.

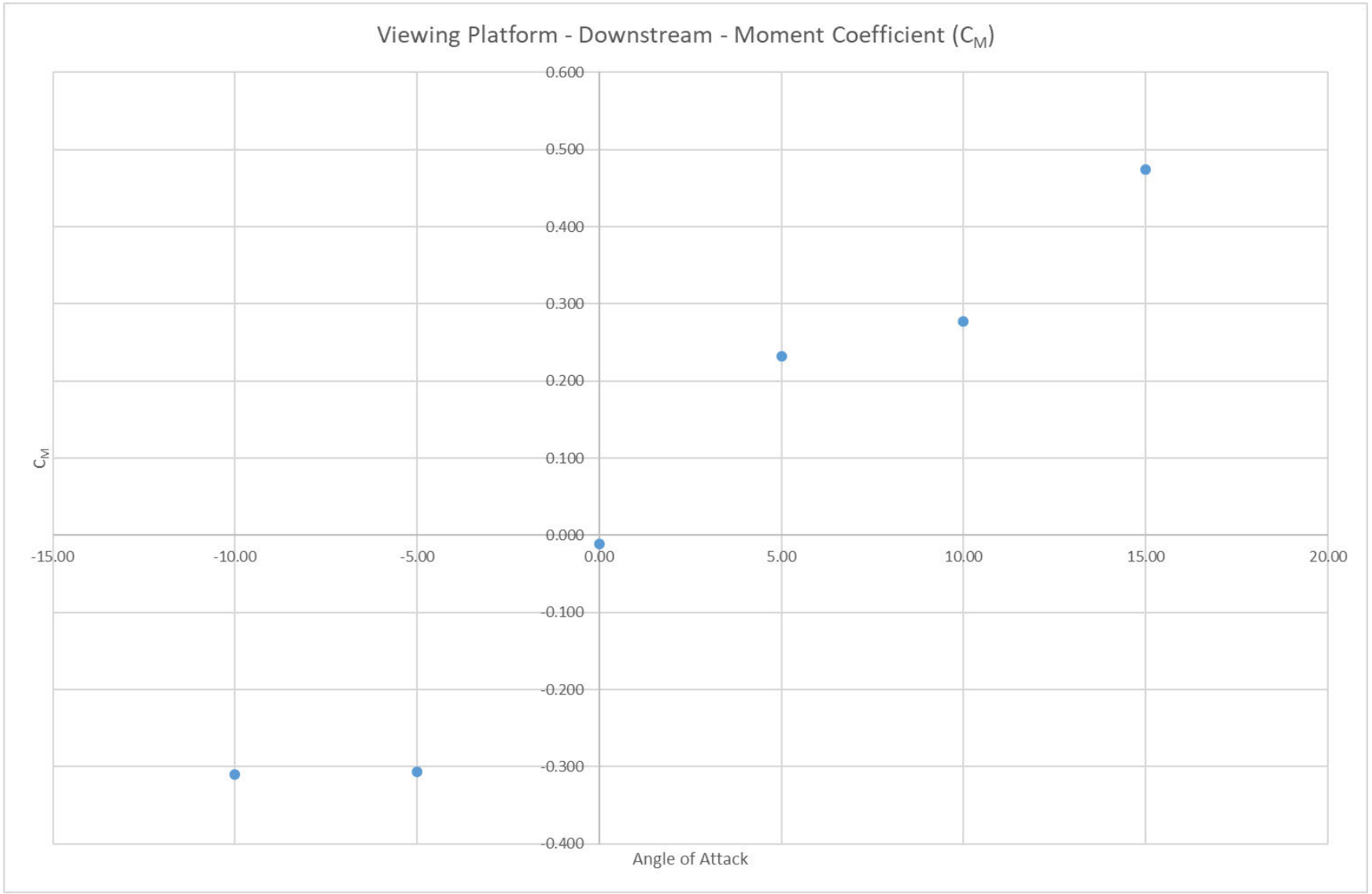

Figure 27: C_M for Section Study 6 of the modified Auckland Harbour Bridge Cycleway as a function of angle of attack.

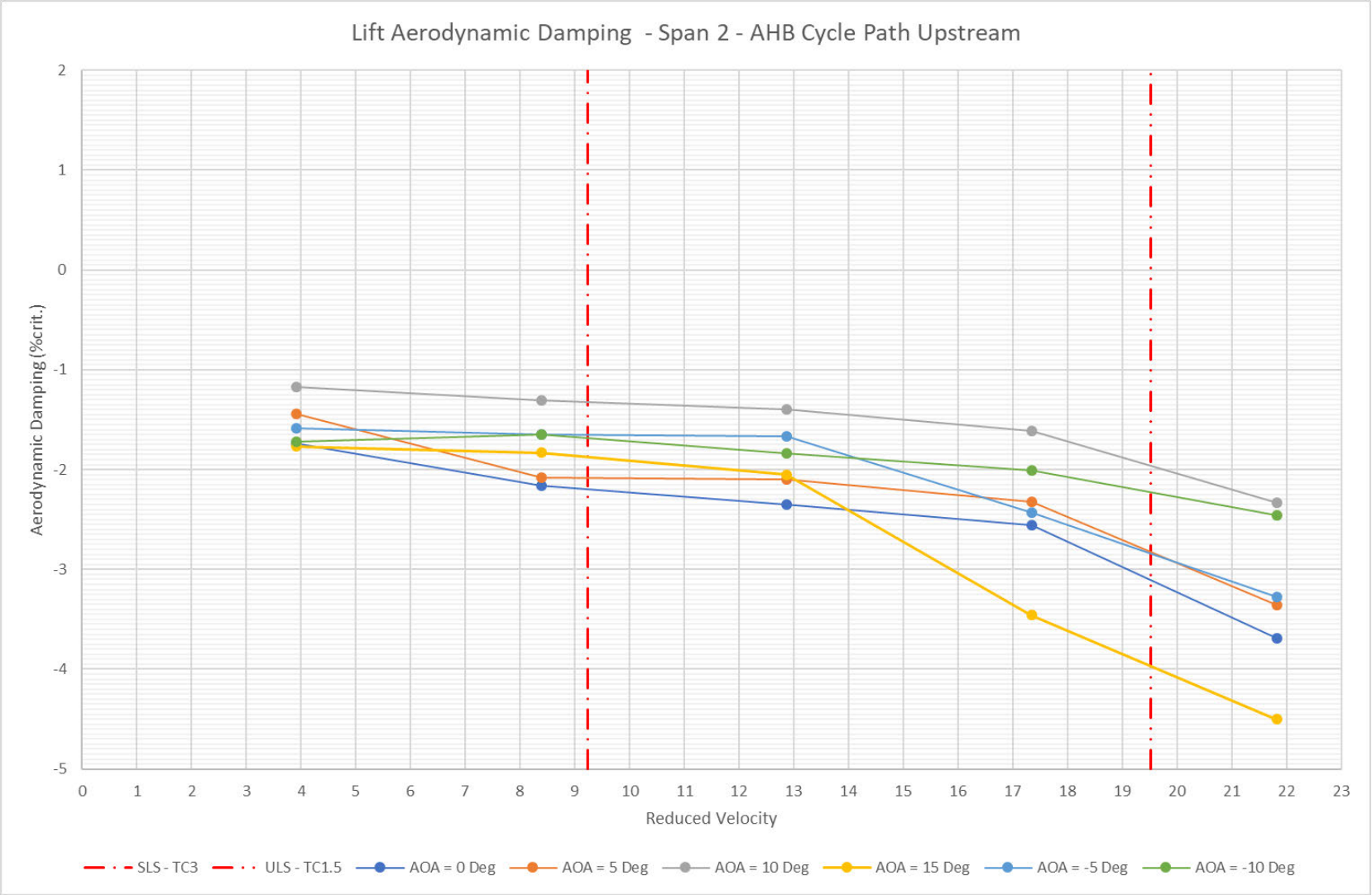

Figure 28: Lift aerodynamic damping for Section Study 1 as a function of Reduced Velocity for the modified Auckland Harbour Bridge Cycleway for a range of angles of attack.

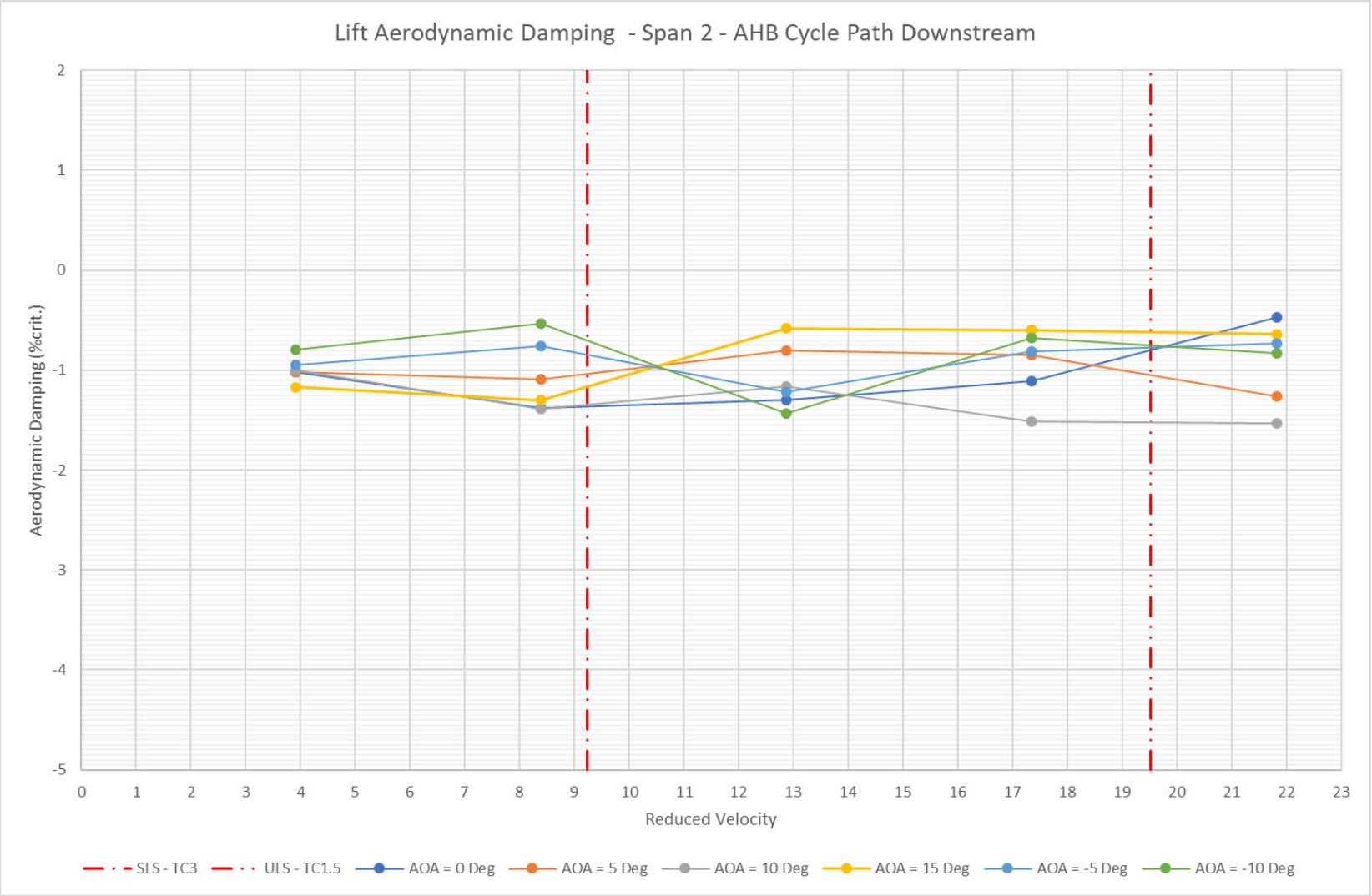

Figure 29: Lift aerodynamic damping for Section Study 2 as a function of Reduced Velocity for the modified Auckland Harbour Bridge Cycleway for a range of angles of attack.

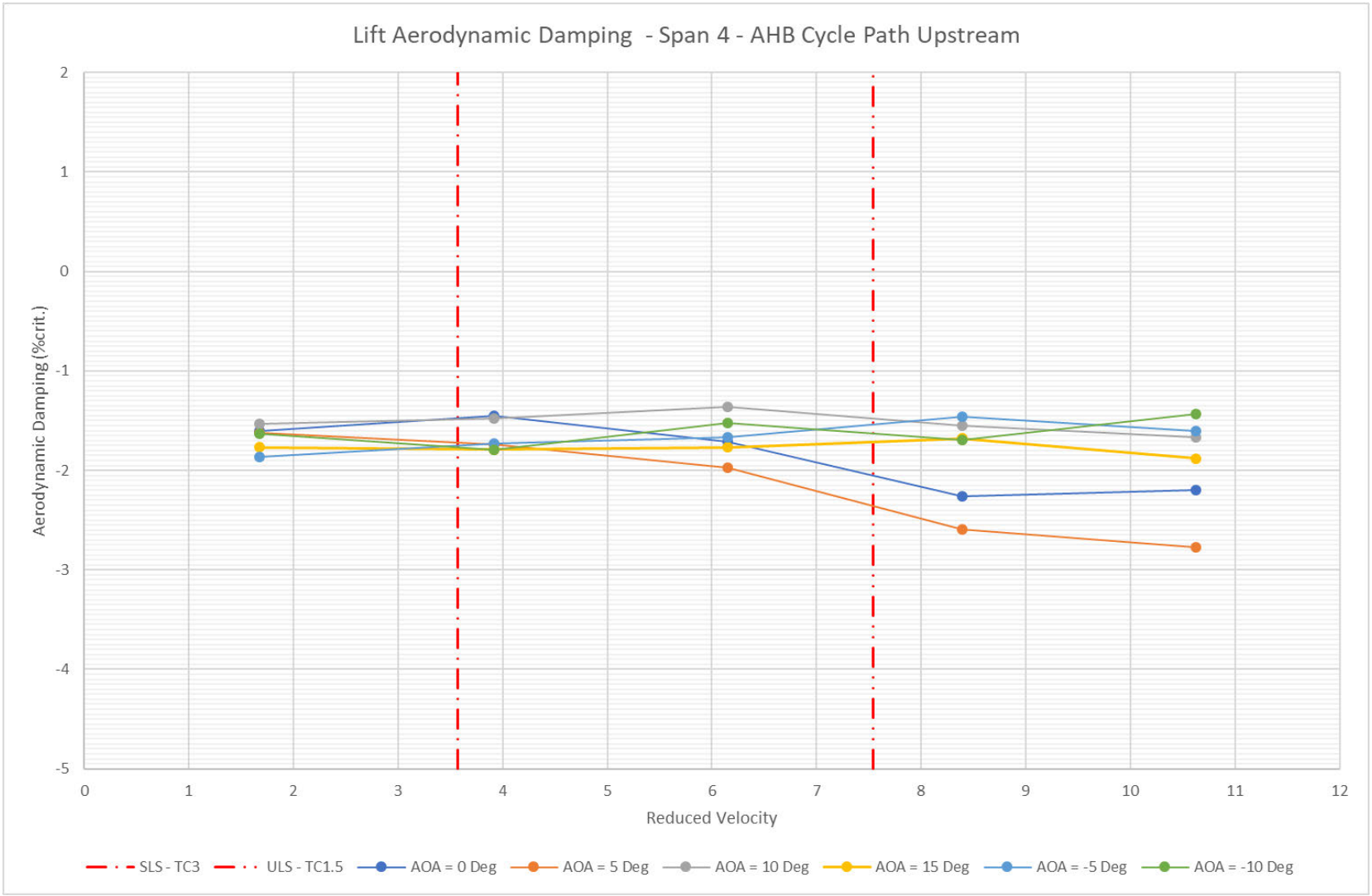

Figure 30: Lift aerodynamic damping for Section Study 3 as a function of Reduced Velocity for the modified Auckland Harbour Bridge Cycleway for a range of angles of attack.

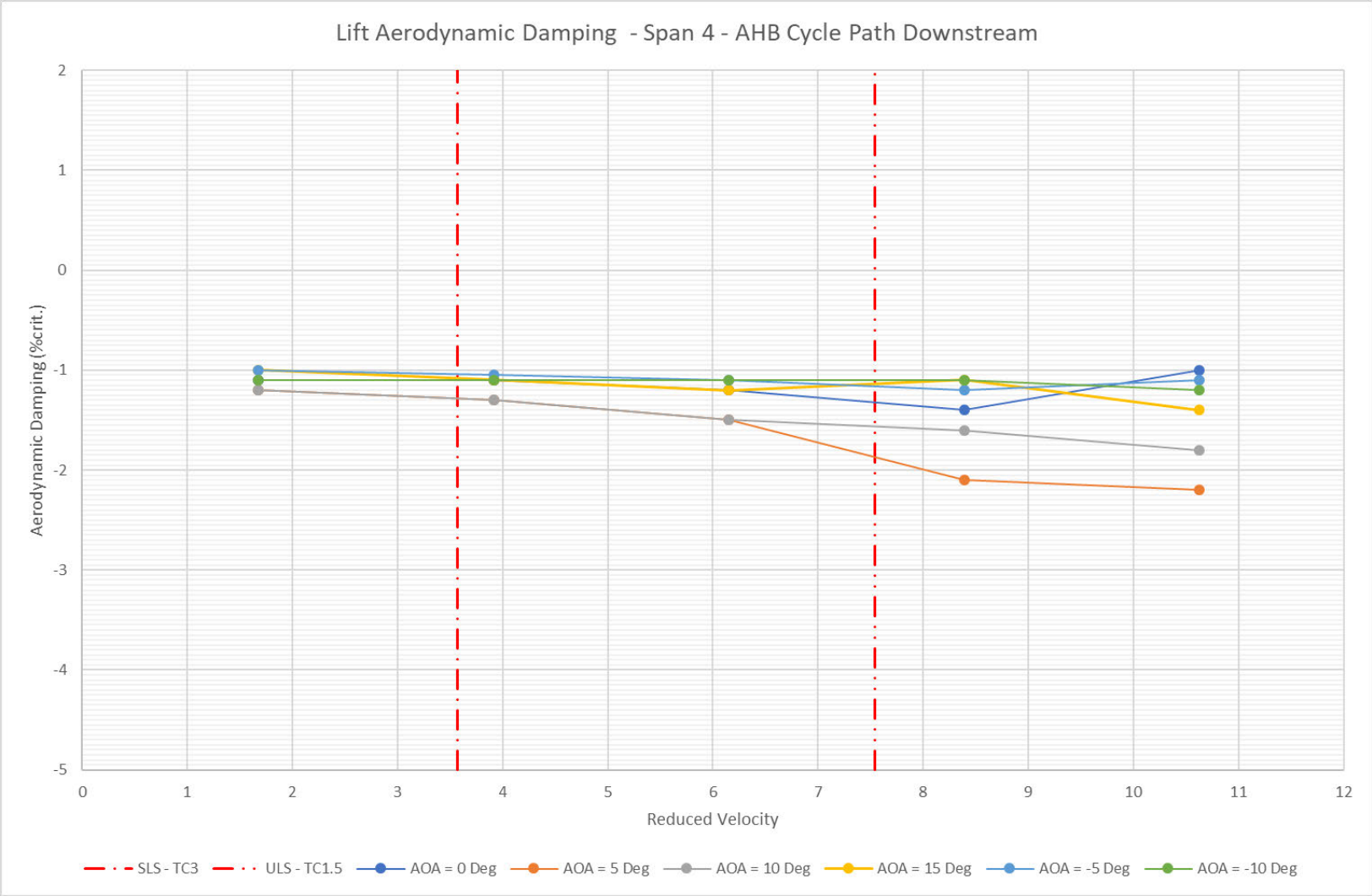

Figure 31: Lift aerodynamic damping for Section Study 4 as a function of Reduced Velocity for the modified Auckland Harbour Bridge Cycleway for a range of angles of attack.